

Collision integral for multigluon production in a scalar quark & gluon model

D. S. Isert and S. P. Klevansky

*Institut für Theoretische Physik,
Philosophenweg 19, D-69120 Heidelberg, Germany*

Abstract

A model of scalar gluons and scalar quarks that successfully gives a $\ln s$ behavior in high energy qq scattering and which contains a three gluon vertex is used to derive transport equations for the quarks and gluons. Quasiparticle and semiclassical approximations are utilized. In particular, the collision integral is studied. At first the terms are organized according to the number of gluon exchange interactions, and it is shown explicitly that the occurrence of all two body differential scattering cross sections in the Boltzmann equation requires an evaluation of *all* terms to this order. One obtains $qg \rightarrow qg$, $q\bar{q} \rightarrow gg$, $qq \rightarrow qq$, and $q\bar{q} \rightarrow q\bar{q}$. An additional ordering according to the inverse number of colors reveals that the quark loop diagrams are suppressed, and diagrams that lead to gluon production or scattering dominate. The self energy with three gluons exchanged is then examined. From this, it is evident that initial as well as final state interactions enter into a generalized collision integral. The generalized Boltzmann-like equation involving n gluon exchange for quark transport is given.

PACS Numbers : 12.40.-y; 05.20.Dd; 12.38.Mh; 24.85.+p.

I. INTRODUCTION

A central issue in describing heavy ion collisions is the question of particle fragmentation, for which there exist several models [1]. From a theoretical point of view, a description of such a collision usually is made within the framework of non-equilibrium theory in which the equation governing the Wigner function that describes the particle distribution $f(X, p)$ semiclassically must somehow be given. From our knowledge of classical systems out of equilibrium and the attendant Boltzmann equations, it is possible to make *heuristic ansätze* for the equations governing the distribution functions of the relevant degrees of freedom. This line of thought has been taken up by several authors in particular from the partonic point of view [2], and, based on this, parton cascade codes have been set up that are successful and necessary for the description of hard processes.

On the other hand, a convincing formal justification of these heuristic ideas using Green function techniques does not yet exist, although steps have been taken in this direction in attempts to derive transport equations directly from the underlying theory of the strong interactions, quantum chromodynamics (QCD), see for example [3–6]. By now, the basic equations of motion for Green functions within a non-equilibrium approach [7–9] for any theory are well known: they can simply be written down in a formal sense; one has a complicated set of matrix Dyson equations relating matrices of Green functions with matrices of self energies, for each particle species. The crux of the issue, after Wigner transformation, is the determination of these self energies for a given theory. The lowest order or mean field contributions to the self energy has been studied in several models of bosons or fermions or both, see for example [10,11]. Higher order terms that contribute to the self energy and which can be interpreted as giving rise to collisional effects are less well studied. Recently, however, it was shown exactly within a simple relativistic model of quarks, the Nambu–Jona-Lasinio model [12], that all graphs that contribute to second order in the interaction are required to generate two body elastic scattering diagrams that contribute to the differential cross-sections occurring in the Boltzmann equation [13].

In this current paper, we study a partonic model of QCD inspired by Polkinghorne [14] that contains scalar quarks and scalar gluons that are coupled to each

other. In addition, the gluons interact with each other via a triple gluon vertex, simulating the non-abelian nature of QCD. Such a 3-gluon vertex turns out to be sufficient to produce “pomeron-like” behavior *i.e.* the quark-quark elastic scattering amplitude can be calculated in a perturbative expansion in leading logarithms of the center of mass energy s , and such an expansion involves only gluonic ladder like diagrams constructed between the two scattering quarks [15]. As it turns out, a 4-gluon vertex would be subleading in the expansion in $\ln s$ and is therefore omitted in this model Lagrangian. We will take this as our starting point. It has the advantage over QCD proper that we can study the consequences of the non-abelian like terms, but we do not have to concern ourselves with the additional problem of gauge invariance [6,16]. There is one additional difficulty, however, that the color structure of the theory becomes necessarily more complicated, but this can be handled relatively easily.

Using the scalar partonic model, we examine the self energies that are required in the non-equilibrium formalism in and beyond the mean field approximation for use in constructing a collision term. Within the mean field approximation, the Hartree term is identically zero, due to color traces. The Fock term, which is often ignored in such calculations¹, is discussed in some detail. The assumption that this term vanishes also, leads to enormous simplifications in considering higher order terms in the coupling g . We then examine the two gluon exchange diagrams, of which there are several different kinds. We classify them according to their topology as being of the “rainbow”, “cloud”, “ladder”, “exchange” or “quark loop” kind. We find that *all* the graphs occurring in this order are required in order to produce the two body partonic differential scattering cross sections that would enter into a Boltzmann-like transport equation, in contrast to that suggested in [4]. This is an exact result. In our case, regarding for example the equations of motion for the quark distribution function, we find that the relevant cross sections that enter into the collision term at this level are either purely quark like in nature ($q\bar{q} \rightarrow q\bar{q}$ and $qq \rightarrow qq$), or contain gluon components ($qg \rightarrow qg$ and $q\bar{q} \rightarrow gg$)². Due to the plethora of different types

¹See however Refs [17] and [18]

²Other processes, such as $q\bar{q}g \rightarrow g$ and $q\bar{q}gg \rightarrow 0$ are suppressed by kinematical

of graphs that already occur at the two gluon exchange level, we seek an additional expansion parameter to simplify this and to enable us to go to higher orders in the coupling. In QCD itself, an expansion in the inverse number of colors is often useful, and we thus examine such an expansion within this model. An analysis of the color structure of each graph naturally suppresses diagrams containing quark loops and the exchange graphs thereof, as is also a feature of QCD. All remaining self energy graphs that contain gluonic exchange components (the ladder, rainbow and cloud graphs) turn out to be superficially of the same order in N_c , and all are required to generate all possible types of gluon production or quark-gluon scattering. A closer look, however, shows that the ratio of the ladder to the rainbow or cloud graphs goes as the ratio of the Casimir operators of the adjoint to the fundamental representations squared, which favors the ladder graphs numerically. The two body process is then briefly reanalysed along these lines.

With this point of view, the next order in the coupling, i.e. the three gluon exchange is investigated. Examining once again the equation of motion for the quark distribution function, we find that three parton production, *i.e.* $q\bar{q} \rightarrow ggg$ and $qg \rightarrow qgg$, naturally occurs. In addition to these production processes, however, the processes $q\bar{q} \rightarrow gg$ and $qgg \rightarrow qg$ must also be accounted for³. We thus see that initial as well as final state processes must be included in the matrix elements. With this information, the generalized Boltzmann equation that includes multiparton production ($q\bar{q} \rightarrow ng$, but also processes of the form $q\bar{q}mg \rightarrow ng$, with m and n integer) within this scalar quark and gluon model is given.

It is to be noted that, unlike the situation that occurs in evaluating the elastic quark-quark scattering amplitude within the scalar parton model [15], we cannot *a priori* make an assumption on the internal ordering of momenta within a self energy graph. This comes about in the elastic quark-quark scattering amplitude, because there are two external momenta that are fixed. In a self energy graph, however, and in the Boltzmann equation, only one external momentum can be fixed while

considerations.

³Again, such processes as $q\bar{q}ggg \rightarrow 0$ and $q\bar{q}gg \rightarrow g$ are suppressed by kinematical considerations.

all the remaining momenta are integrated over. Thus the simplifications leading to the ladder approximation and Regge behavior in that calculation are not simply recovered in the kinetic theory.

This paper is organized as follows. In Section II, we give a brief introduction to the scalar partonic model, and set our notation for the nonequilibrium dynamics. In Section III, we describe the collisional contributions that arise from the mean field self energies, and the associated transport equations. In Section IV, we deal with the collision integral beyond the mean field approach, firstly giving the exact perturbative calculations with two gluon exchange, the color expansion, then three and n gluon exchange. We summarize and conclude in Section V.

II. MODEL OF SCALAR QUARKS AND GLUONS, AND TRANSPORT THEORY

In this section, we introduce and discuss the scalar partonic model, and give the equations of motion for quark and gluon fields. We then give a brief discussion of transport theory applied to this scalar model, and indicate the self energies that we are required to evaluate.

A. Scalar partonic model

In the model underpinning our calculations, quarks and antiquarks are described by complex scalar fields ϕ , and gluons as the scalar field χ coupled through the Lagrangian

$$\begin{aligned} \mathcal{L} = & \partial^\mu \phi^{\dagger i, l} \partial_\mu \phi_{i, l} + \frac{1}{2} \partial^\mu \chi_{a, r} \partial_\mu \chi^{a, r} - \frac{m^2}{2} \chi_{a, r} \chi^{a, r} \\ & - g m \phi^{\dagger i, l} (T^a)_i^j (T^r)_l^m \phi_{j, m} \chi_{a, r} - \frac{g m}{3!} f_{abc} f_{rst} \chi^{a, r} \chi^{b, s} \chi^{c, t}. \end{aligned} \quad (2.1)$$

The quark fields are regarded as massless, as one generally assumes for high energy processes, while the gluons are usually assigned a mass m *a priori* in order to avoid infra-red divergences. There is an interaction between quarks and gluons as well as a cubic self-interaction between gluons. Since in QCD the quartic interaction between gluons leads to terms which are sub-leading in $\ln s$, such a quartic interaction among gluons is not included within this model.

One notes that both the quark and gluon fields carry two labels. Both of these refer to color groups. The fact that a direct product of two color groups is necessary can be seen on examining the three gluon vertex term. This term must be symmetric under the exchange of two gluons since they are bosons. In addition, one expects that the interaction vertex should be proportional to the (antisymmetric) structure constants of the color group. A single color group cannot meet these requirements, and the simplest combination which can is a product of two $SU(N_c)$ groups. Thus the gluon field carries two color indices ($a, r = 1 \dots (N_c^2 - 1)$). Since the quark field transforms in the fundamental representation of both of these $SU(N_c)$ groups, it must carry two color indices as well ($i, l = 1 \dots N_c$). The matrices T^a and T^r are the generators and f_{abc} and f_{rst} are the structure constants for the two $SU(N)$ groups respectively. Thus they satisfy

$$[T^a, T^b] = if_{abc}T^c, \quad [T^r, T^s] = if_{rst}T^t. \quad (2.2)$$

Note in Eq.(2.1) that the flavor index of the quark fields is suppressed.

The equations of motion for the fields can be derived from the Euler-Lagrange equations. They are

$$\square \phi^{(\dagger)i,l} = -gm(T^a)_j^i (T^r)_m^l \phi^{(\dagger)j,m} \chi_{a,r} \quad (2.3)$$

for the (anti-)quarks and

$$(\square + m^2)\chi^{a,r} = -gm[\phi^{\dagger i,l}(T^a)_j^i (T^r)_l^m \phi_{j,m} + f^{abc} f^{rst} \chi_{b,s} \chi_{c,t}] \quad (2.4)$$

for the gluons.

B. Transport theory for interacting bosonic fields

For the purpose of establishing our notation, we give the basic definitions and refer the reader to standard texts [7–9]. The quark Green functions in the Schwinger-Keldysh formalism [19] are defined as

$$\begin{aligned} iS^c(x, y) &= \langle T \phi^{i,l}(x) \phi^{\dagger j,m}(y) \rangle - \langle \phi^{i,l}(x) \rangle \langle \phi^{\dagger j,m}(y) \rangle = iS^{--}(x, y) \\ iS^a(x, y) &= \langle \tilde{T} \phi^{i,l}(x) \phi^{\dagger j,m}(y) \rangle - \langle \phi^{i,l}(x) \rangle \langle \phi^{\dagger j,m}(y) \rangle = iS^{++}(x, y) \\ iS^>(x, y) &= \langle \phi^{i,l}(x) \phi^{\dagger j,m}(y) \rangle - \langle \phi^{i,l}(x) \rangle \langle \phi^{\dagger j,m}(y) \rangle = iS^{+-}(x, y) \\ iS^<(x, y) &= \langle \phi^{\dagger j,m}(y) \phi^{i,l}(x) \rangle - \langle \phi^{i,l}(x) \rangle \langle \phi^{\dagger j,m}(y) \rangle = iS^{-+}(x, y) \end{aligned} \quad (2.5)$$

and for the gluons as

$$\begin{aligned}
iG^c(x, y) &= \langle T\chi^{a,r}(x)\chi^{b,s}(y) \rangle - \langle \chi^{a,r}(x) \rangle \langle \chi^{b,s}(y) \rangle = iG^{--}(x, y) \\
iG^a(x, y) &= \langle \tilde{T}\chi^{a,r}(x)\chi^{b,s}(y) \rangle - \langle \chi^{a,r}(x) \rangle \langle \chi^{b,s}(y) \rangle = iG^{++}(x, y) \\
iG^>(x, y) &= \langle \chi^{a,r}(x)\chi^{b,s}(y) \rangle - \langle \chi^{a,r}(x) \rangle \langle \chi^{b,s}(y) \rangle = iG^{+-}(x, y) \\
iG^<(x, y) &= \langle \chi^{b,s}(y)\chi^{a,r}(x) \rangle - \langle \chi^{a,r}(x) \rangle \langle \chi^{b,s}(y) \rangle = iG^{-+}(x, y).
\end{aligned} \tag{2.6}$$

Here T and \tilde{T} are the usual time and anti-time ordering operators respectively. As given, the Green functions fall along the contour designated in Fig. 1. Our convention follows that of Ref. [9]. They satisfy a Dyson equation that introduces the matrix of self energies for either the quark or gluonic sectors, $\underline{\Sigma}_q$ or $\underline{\Sigma}_g$. Using a generic notation, $\underline{D} = \underline{S}$ or \underline{G} and $\underline{\Pi} = \underline{\Sigma}_q$ or $\underline{\Sigma}_g$ as appropriate, one may write

$$\begin{aligned}
\underline{D}(x, y) &= \underline{D}^0(x, y) - \int d^4z d^4w \underline{D}^0(x, w) \underline{\Pi}(w, z) \underline{D}(z, y) \\
&= \underline{D}^0(x, y) - \int d^4z d^4w \underline{D}(x, w) \underline{\Pi}(w, z) \underline{D}^0(z, y).
\end{aligned} \tag{2.7}$$

In a standard fashion, the transport and constraint equations can be derived, and this is summarized briefly in Appendix A. In terms of the center of mass variable $X = x + y$ and the Fourier transform variable p conjugate to the relative distance $u = x - y$, or Wigner transform, the equations that one obtains for the off diagonal Green functions, corresponding to the transport and constraint equations are

$$-2ip\partial_X D^{-+}(X, p) = I_- \quad \text{transport} \tag{2.8}$$

and

$$\left(\frac{1}{2}\square_X - 2p^2 + 2M^2\right) D^{-+}(X, p) = I_+, \quad \text{constraint} \tag{2.9}$$

respectively, where M is a generic parton mass, $M = m$ for the gluons and $M = 0$ for the quarks. I_{\mp} is an abbreviation for the combined functions

$$I_{\mp} = I_{\text{coll}} + I_{\mp}^A + I_{\mp}^R, \tag{2.10}$$

and I_{coll} is the collision term,

$$\begin{aligned}
I_{\text{coll}} &= \Pi^{-+}(X, p) \hat{\Lambda} D^{+-}(X, p) - \Pi^{+-}(X, p) \hat{\Lambda} D^{-+}(X, p) \\
&= I_{\text{coll}}^{\text{gain}} - I_{\text{coll}}^{\text{loss}}.
\end{aligned} \tag{2.11}$$

I_{\mp}^R and I_{\mp}^A are terms containing retarded and advanced components respectively,

$$I_{\mp}^R = -\Pi^{-+}(X, p)\hat{\Lambda}D^R(X, p) \pm D^R(X, p)\hat{\Lambda}\Pi^{-+}(X, p) \quad (2.12)$$

and

$$I_{\mp}^A = \Pi^A(X, p)\hat{\Lambda}D^{-+}(X, p) \mp D^{-+}(X, p)\hat{\Lambda}\Pi^A(X, p). \quad (2.13)$$

In Eqs.(2.11) to (2.13), the operator $\hat{\Lambda}$ is given by

$$\hat{\Lambda} := \exp \left\{ \frac{-i}{2} \left(\overleftarrow{\partial}_X \overrightarrow{\partial}_p - \overleftarrow{\partial}_p \overrightarrow{\partial}_X \right) \right\}. \quad (2.14)$$

In order to proceed further, we have to calculate the self energies. It is useful to introduce the quasiparticle approximation, in which a *free* scalar parton of mass M is assigned the Green functions

$$iD^{-+}(X, p) = \frac{\pi}{E_p} \{ \delta(E_p - p^0) f_a(X, p) + \delta(E_p + p^0) \bar{f}_a(X, -p) \} \quad (2.15)$$

$$iD^{+-}(X, p) = \frac{\pi}{E_p} \{ \delta(E_p - p^0) \bar{f}_a(X, p) + \delta(E_p + p^0) f_a(X, -p) \} \quad (2.16)$$

$$\begin{aligned} iD^{--}(X, p) &= \frac{i}{p^2 - M^2 + i\epsilon} + \Theta(-p^0)D^{+-}(X, p) + \Theta(p^0)D^{-+}(X, p) \\ &= \frac{i}{p^2 - M^2 + i\epsilon} + \frac{\pi}{E_p} \{ \delta(E_p - p^0) f_a(X, p) + \delta(E_p + p^0) \bar{f}_a(X, -p) \} \end{aligned} \quad (2.17)$$

$$\begin{aligned} iD^{++}(X, p) &= \frac{-i}{p^2 - M^2 - i\epsilon} + \Theta(-p^0)D^{+-}(X, p) + \Theta(p^0)D^{-+}(X, p) \\ &= \frac{-i}{p^2 - M^2 - i\epsilon} + \frac{\pi}{E_p} \{ \delta(E_p - p^0) f_a(X, p) + \delta(E_p + p^0) \bar{f}_a(X, -p) \} \end{aligned} \quad (2.18)$$

with $E_p^2 = p^2 + M^2$, and which are given in terms of the corresponding scalar quark and gluon distribution function, $f_a(X, p)$, and $\bar{f}_a = 1 + f_a$, where a denotes the parton type $a = q, g$.

Our task in this paper is to construct an equation for the distribution functions for quarks and gluons $f_a(X, p)$ from Eqs.(2.8) to (2.13), using the quasiparticle Green functions of the form given in Eqs.(2.15) to (2.18). To do so, it is necessary to integrate the entire Eq.(2.8) over an interval Δ_{\pm} which contains $\pm E_p(X)$. Our particular focus will be placed on the collision terms that are derived from Eq.(2.11). In anticipation of this fact, we will require such an integration over the terms appearing in Eq.(2.11), and define

$$\begin{aligned}
J_{\text{coll}} &= J_{\text{coll}}^{\text{gain}} - J_{\text{coll}}^{\text{loss}} \\
&= \int_{\Delta^+} dp_0 I_{\text{coll}}^{\text{gain}} - \int_{\Delta^+} dp_0 I_{\text{coll}}^{\text{loss}}.
\end{aligned} \tag{2.19}$$

To lowest order in an expansion that sets $\hat{\Lambda} = 1$, this integral can be easily performed. One has

$$\begin{aligned}
J_{\text{coll}} &= \int_{\Delta^+} dp_0 \Pi^{-+}(X, p) D^{+-}(X, p) - \int_{\Delta^+} dp_0 \Pi^{+-}(X, p) D^{-+}(X, p) \\
&= -i \frac{\pi}{E_p} \Pi^{-+}(X, p_0 = E_p, \vec{p}) \bar{f}_a(X, \vec{p}) + i \frac{\pi}{E_p} \Pi^{+-}(X, p_0 = E_p, \vec{p}) f_a(X, \vec{p}),
\end{aligned} \tag{2.20}$$

i.e. the off-diagonal quasiparticle self energies are required to be calculated on shell.

III. THE COLLISION INTEGRAL - MEAN FIELD SELF ENERGIES

In this section, we evaluate the self energies to first order in the interaction strength and illustrate their role in the transport equation in the semi-classical limit.

A. Hartree self energies

For the scalar parton model, two generic kinds of Hartree graphs can be identified in the quark and gluon self energies. These are depicted in Fig. 2. For Hartree diagrams of any kind, off diagonal self energies are per definition zero and only diagonal elements can possibly be constructed, *i.e.* Σ_H^{--} or Σ_H^{++} . However, all such diagrams vanish identically in this model. The reason for this lies in the color factors: for the quark self energy graph in Fig. 2 that contains a quark loop, a single SU(3) color group leads to the associated color factor

$$F_{H,q} = t_{ii}^a \text{tr}(t^a) = 0, \tag{3.1}$$

since $t_a = \lambda^a/2$, where λ^a are the Gell-Mann matrices. In the above expression, i denotes the external quark momentum and is therefore not to be summed over. For the quark self energy containing a gluon line, the color factor for a single SU(3) group is also vanishing,

$$F_{H,g} = t_{ii}^a T_{bb}^a = -it_{ii}^a f_{abb} = 0. \quad (3.2)$$

Similar arguments apply to the gluon self energies. Thus, no mass renormalization occurs due to Hartree terms.

A semiclassical expansion of the transport and constraint equations thus leads to free streaming described by

$$-2ip\partial_X D^{-+}(X, p) = 0, \quad (3.3)$$

and the constraint equation is

$$(p^2 - M^2)D^{-+}(X, p) = 0. \quad (3.4)$$

By integrating Eq.(3.3) over a positive interval Δ_+ , the equations for the time evolution of the distribution function for quarks and gluons emerge,

$$p\partial_X f_a(X, p) = 0, \quad (3.5)$$

with $p^\mu = (E_p, \vec{p})$. On integrating the constraint equation, Eq.(3.4), one has $(E_p^2 - \vec{p}^2 - M^2)f_a(X, p) = 0$. The equation is the expression of the fact that the partons have to be on mass-shell, and is consistent with the quasiparticle assumption, Eqs.(2.15) - (2.18) made in the first place.

B. Fock self energies

The next type of graph contributing to the mean field expansion is the Fock term. The generic diagrams for the quark and gluon self energies are shown in Fig. 3⁴.

Since we are particularly concerned with the collision integral, we start with the quark sector and examine as an example, the gain term generated by the Fock term $\Sigma_{F,q}^{-+}(X, p)$. By inspection, one has

$$i\Sigma_{F,q}^{-+}(X, p) = -g^2 m^2 F_{F,q}^2 \int \frac{d^4 p_1}{(2\pi)^4} \int \frac{d^4 p_2}{(2\pi)^4} S^{-+}(X, p_1) G^{+-}(X, p_2) (2\pi)^4 \delta^{(4)}(p - p_1 + p_2), \quad (3.6)$$

⁴Fig.3(b) is strictly speaking a vacuum polarization graph for the gluons

and $F_{F,q}$ is the Fock color factor for a single $SU(N_c)$ group,

$$F_{F,q} = t_{ij}^a t_{ji}^a = \frac{N_c^2 - 1}{2N_c} \delta_{ii}. \quad (3.7)$$

The contribution to the collision term that this makes, using Eqs.(2.19) and (2.20) is

$$J_{F,\text{coll}}^{\text{gain}} = \int_{\Delta_+} dp^0 \Sigma_{F,q}^{-+}(X, p) \left(-\frac{i\pi}{E_p}\right) \delta(p_0 - E_p) \bar{f}_q(X, p), \quad (3.8)$$

which, on inserting the explicit expressions for $S^{-+}(X, p)$ and $G^{+-}(X, p)$ from Eqs.(2.15) and (2.16) leads to four distinct terms,

$$\begin{aligned} J_{F,\text{coll}}^{\text{gain}} = & -g^2 m^2 F_F^2 \frac{\pi}{E_p} \int_{\Delta_+} dp^0 \delta(E_p^q - p^0) \int \frac{d^4 p_1}{(2\pi)^4} \int \frac{d^4 p_2}{(2\pi)^4} (2\pi)^4 \delta^{(4)}(p + p_1 - p_2) \\ & \times \frac{\pi}{E_1} \frac{\pi}{E_2} \sum_{i=1}^4 T_i, \end{aligned} \quad (3.9)$$

where

$$\begin{aligned} T_1 &= \delta(E_1 - p_1^0) \delta(E_2 - p_2^0) \bar{f}_{\bar{q}}(X, p_1) f_g(X, p_2) \bar{f}_q(X, p) \\ T_2 &= \delta(E_1 - p_1^0) \delta(E_2 + p_2^0) \bar{f}_{\bar{q}}(X, p_1) \bar{f}_g(X, -p_2) \bar{f}_q(X, p) \\ T_3 &= \delta(E_1 + p_1^0) \delta(E_2 + p_2^0) f_q(X, -p_1) \bar{f}_g(X, -p_2) \bar{f}_q(X, p) \\ T_4 &= \delta(E_1 + p_1^0) \delta(E_2 - p_2^0) f_q(X, -p_1) f_g(X, p_2) \bar{f}_q(X, p). \end{aligned} \quad (3.10)$$

By attributing unbarred functions f to incoming particles and barred functions \bar{f} to outgoing ones, one can see that $T_1..T_4$ correspond to the processes $g \rightarrow q\bar{q}$, $\emptyset \rightarrow q\bar{q}g$, $q \rightarrow qg$ and $qg \rightarrow q$. The last three of these are kinematically forbidden, while the former is possible, since the gluons are endowed with a finite mass. Performing the integrals over p_1^0 and p_2^0 , Eq.(3.10) becomes

$$\begin{aligned} \int_{\Delta_+} dp^0 \Sigma_{F,q}^{-+}(X, p) S^{+-}(X, p) = & -\frac{\pi}{E_p} \int \frac{d^3 p_1}{(2\pi)^3 2E_1} \frac{d^3 p_2}{(2\pi)^3 2E_2} (2\pi)^4 \delta^{(4)}(p + p_1 - p_2) \\ & \times |\mathcal{M}|_{g \rightarrow q\bar{q}}^2 f_g(X, p_2) \bar{f}_{\bar{q}}(X, p_1) \bar{f}_q(X, p). \end{aligned} \quad (3.11)$$

The loss term is obtained in a similar fashion or by exchanging f with \bar{f} , since the matrix element is symmetric. Combining both terms, the revised transport equation is obtained on integrating Eq.(2.11) over the energy interval Δ_+ as

$$\begin{aligned}
2p\partial_X f_q(X, p) &= \int \frac{d^3 p_1}{(2\pi)^3 2E_1} \frac{d^3 p_2}{(2\pi)^3 2E_2} (2\pi)^4 \delta^{(4)}(p + p_1 - p_2) \\
&\times |\mathcal{M}|_{g \rightarrow q\bar{q}}^2 [f_g(X, p_2) \bar{f}_{\bar{q}}(X, p_1) \bar{f}_q(X, p) - \bar{f}_g(X, p_2) f_q(X, p_1) f_q(X, p)].
\end{aligned} \tag{3.12}$$

This is the final expression for the Fock transport equation. One can alternatively introduce a cosmetic recombination or decay rate in which case Eq.(3.12) can be written symbolically as

$$\begin{aligned}
2p\partial_X f_q(X, p) &= \int \frac{d^3 p_2}{(2\pi)^3 2E_2} \int d\Omega \frac{d\sigma}{d\Omega} \Big|_{q\bar{q} \rightarrow g} F \\
&\times [f_g(X, p_2) \bar{f}_{\bar{q}}(X, p_1) \bar{f}_q(X, p) - \bar{f}_g(X, p_2) f_q(X, p_1) f_q(X, p)],
\end{aligned} \tag{3.13}$$

where F is the flux factor, and

$$\int d\Omega \frac{d\sigma}{d\Omega} = \int dQ \frac{|\mathcal{M}|^2}{F} \tag{3.14}$$

with the invariant phase space factor dQ given as $dQ = (2\pi)^4 \delta^{(4)}(p + p_1 - p_2) d^3 p_2 / ((2\pi)^3 2E_2)$.

An analysis of the self energy graph 3(a) of the gluon sector, $\Sigma_{F,g(a)}^{-+}(X, p)$ along the previous lines leads to processes $g \rightarrow gg$, $\emptyset \rightarrow ggg$, and $gg \rightarrow g$, all of which are kinematically prohibited. One thus obtains

$$(J_{F, \text{gain/loss}}^{\text{coll}(a)})_{\text{gluonic graph}} = 0. \tag{3.15}$$

This can be attributed to the fact that the self energies are evaluated on shell, i.e. we may write

$$\Sigma_{F,g(a)}^{-+}(X, p_0 = E_p, \vec{p}) = \Sigma_{F,g(a)}^{+-}(X, p_0 = E_p, \vec{p}) = 0, \tag{3.16}$$

which is the statement that an on shell particle cannot decay into two on shell particles of the same kind.

The second graph in the gluonic case does not vanish. This self energy $\Sigma_{F,g(b)}^{-+}$ that enters into the description of the gain in gluons, is precisely that given in Eq.(3.6), but with $G^{+-}(X, p_2)$ replaced by $S^{+-}(X, p_2)$. The color factor in this case is also modified, being $F_{F,g} = 1/2\delta^{aa}$. An analysis of the self energy along the same lines leads to the processes $q \rightarrow qg$, $\bar{q} \rightarrow \bar{q}g$, $\emptyset \rightarrow gq\bar{q}$ and $q\bar{q} \rightarrow g$, the last of which is the

only term that can contribute. Thus the time evolution of the gluon distribution function is given by

$$\begin{aligned}
2p\partial_X f_g(X, \vec{p}) = & \int \frac{d^3 p_1}{(2\pi)^3 2E_1} \frac{d^3 p_2}{(2\pi)^3 2E_2} (2\pi)^4 \delta^{(4)}(p + p_1 - p_2) \\
& \times |\mathcal{M}|_{g \rightarrow q\bar{q}}^2 [f_q(X, p_2) \bar{f}_{\bar{q}}(X, p_1) \bar{f}_g(X, p) - \bar{f}_q(X, p_2) \bar{f}_{\bar{q}}(X, p_1) f_g(X, p)].
\end{aligned}
\tag{3.17}$$

We conclude this section by commenting the result that while the Fock term 3(a) for gluons vanishes identically, the Fock term for the quark self energy does not. A term of this kind occurs in this model because the quarks are massless, while the gluons are massive. The relevance of this Fock term thus depends on the form of the underlying theory. In evaluating higher order graphs in the following section, it is useful to invoke the so-called “on-shell argument”, ignoring all terms of higher order of this kind that contain on-shell decays. This is necessary in order to render the problem tractable, but it is not strictly true, as has been indicated here.

IV. THE COLLISION INTEGRAL - BEYOND THE MEAN FIELD

A. Exact perturbative calculations that contain two loops

Generic diagrams that contain two loops and which contribute to the quark and gluon sectors are shown in Fig. 4. In the quark sector, we denote these graphs as rainbow (R), ladder (L), cloud (C), exchange (E) and quark loop graphs (q-Loop), according to their topology. These graphs comprise all diagrams with two exchanged gluons. In the gluonic sector, there are more diagrams, as can be seen in the figure. Note that in this sector, a ladder-like diagram is topologically equivalent to the rainbow kind, and is therefore not included separately. Since we are specifically interested in the collisional term, we will concern ourselves only with the off-diagonal contributions that arise from these diagrams, as is required in Eq.(2.11). In addition, these self energies are required on shell.

To be specific, let us deal first with the quark sector, and consider the rainbow diagram first. Then there are four possibilities of ordering the lines in this graph, as is indicated in Fig. 5. However, invoking the on-shell argument, as explained in the previous section for the Fock diagram, only the first graph of this series can survive

while the other three vanish. Similar arguments can be applied to the remaining graphs, the L, C, E, and q-Loop diagrams. One can set up all possibilities of ordering the lines for each type of graph in Fig. 4, and determine which survive. The final set of all non-vanishing contributions can then be ascertained. These are shown in Fig. 6.

We next note that the diagram of Fig. 6.4(b) is the exchange graph of Fig. 6.5, because both of these diagrams contain three off-diagonal quark Green functions. The similarity becomes more evident if one redraws the diagram of Fig. 6.4(b) as shown in Fig. 7.

The self energies for two gluon exchange contribute to the quark collision term via

$$\begin{aligned} J_{\text{coll}}^{(2)} &= \int_{\Delta^+} dp_0 \Sigma^{(2)-+}(X, p) S^{+-}(X, p) - \int_{\Delta^+} dp_0 \Sigma^{(2)+-}(X, p) S^{-+}(X, p) \\ &= -i \frac{\pi}{E_p} \Sigma^{(2)-+}(X, p_0 = E_p, \vec{p}) \bar{f}_q(X, \vec{p}) + i \frac{\pi}{E_p} \Sigma^{(2)+-}(X, p_0 = E_p, \vec{p}) f_q(X, \vec{p}), \end{aligned} \quad (4.1)$$

where the off-diagonal self energies are constructed from the diagrams of Fig. 4 as

$$\Sigma^{(2)\pm\mp}(X, p) = \Sigma_{\text{quark-quark}}^{(2)\pm\mp}(X, p) + \Sigma_{\text{quark-gluon}}^{(2)\pm\mp}(X, p) \quad (4.2)$$

where

$$\Sigma_{\text{quark-quark}}^{(2)+-}(X, p) = \Sigma_{E,b}^{(2)+-}(X, p) + \Sigma_{\text{q-Loop}}^{(2)+-}(X, p) \quad (4.3)$$

and

$$\begin{aligned} \Sigma_{\text{quark-gluon}}^{(2)+-}(X, p) &= \Sigma_R^{(2)+-}(X, p) + \Sigma_L^{(2)+-}(X, p) + \Sigma_{C,a}^{(2)+-}(X, p) \\ &\quad + \Sigma_{C,b}^{(2)+-}(X, p) + \Sigma_{E,a}^{(2)+-}(X, p). \end{aligned} \quad (4.4)$$

Here we have split up the combinations of the second exchange plus quark loop diagrams in $\Sigma_{\text{quark-quark}}$, leaving the rainbow, cloud, ladder and first exchange graph to $\Sigma_{\text{quark-gluon}}$. This subdivision in Eqs.(4.3) and (4.4) to $J_{\text{coll}}^{(2)}$ in Eq.(4.1) will be handled separately, as the first term will be seen to lead to elastic quark-quark and quark-antiquark differential scattering cross sections in the transport equation, while the $\Sigma_{\text{quark-gluon}}$ term will be seen to lead to processes involving gluons in the final state, such as the processes $q\bar{q} \rightarrow gg$ and $qg \rightarrow qg$.

1. *Quark-quark and quark-antiquark scattering cross sections.*

Explicit expressions for the quark loop and its exchange diagram self energies required in Eq.(4.3) are obtained as

$$\begin{aligned}\Sigma_{\text{q-Loop}}^{(2)+-}(X, p) = & -g^4 m^4 F_{\text{q-Loop}}^2 \int \frac{d^4 p_1}{(2\pi)^4} \frac{d^4 p_2}{(2\pi)^4} \frac{d^4 p_3}{(2\pi)^4} \frac{d^4 p_4}{(2\pi)^4} (2\pi)^4 \delta^{(4)}(p - p_1 - p_2) \\ & \times (2\pi)^4 \delta^{(4)}(p_2 - p_3 + p_4) S^{+-}(X, p_1) G^{++}(X, p_2) \\ & \times S^{+-}(X, p_3) S^{-+}(X, p_4) G^{--}(X, p_2)\end{aligned}\quad (4.5)$$

and

$$\begin{aligned}\Sigma_{E,b}^{(2)+-}(X, p) = & -g^4 m^4 F_E^2 \int \frac{d^4 p_1}{(2\pi)^4} \frac{d^4 p_2}{(2\pi)^4} \frac{d^4 p_3}{(2\pi)^4} \frac{d^4 p_4}{(2\pi)^4} (2\pi)^4 \delta^{(4)}(p - p_1 - p_2) \\ & \times (2\pi)^4 \delta^{(4)}(p_2 - p_3 + p_4) S^{+-}(X, p_1) G^{++}(X, p_2) \\ & \times S^{+-}(X, p_3) S^{-+}(X, p_4) G^{--}(X, p - p_3),\end{aligned}\quad (4.6)$$

where $F_{\text{q-Loop}}$ and F_E are color factors, that will be given explicitly in the following subsection. Since they do not affect our argument, we suppress them in the following.

The integrated collision term, for loss, for example, from Eq.(4.1) can be directly evaluated, to give the quark loop and exchange contributions

$$\begin{aligned}J_{\text{coll,q}}^{(2)\text{loss}} = & ig^4 m^4 \frac{\pi}{E_p} \int \frac{d^4 p_1}{(2\pi)^4} \frac{d^4 p_2}{(2\pi)^4} \frac{d^4 p_3}{(2\pi)^4} \frac{d^4 p_4}{(2\pi)^4} (2\pi)^8 \delta^{(4)}(p - p_1 - p_2) \delta^{(4)}(p_2 - p_3 + p_4) \\ & \times \left\{ G^{++}(X, p_2) G^{--}(X, p_2) + G^{++}(X, p_2) G^{--}(X, p - p_3) \right\} \\ & \times \left(-i \frac{\pi}{E_1} \right) \left(-i \frac{\pi}{E_3} \right) \left(-i \frac{\pi}{E_4} \right) \sum_{i=1}^8 T_i,\end{aligned}\quad (4.7)$$

where

$$\begin{aligned}T_1 = & \delta(E_1 + p_1^0) \delta(E_3 + p_3^0) \delta(E_4 + p_4^0) f_{\bar{q}}(-p_1) f_{\bar{q}}(-p_3) \bar{f}_{\bar{q}}(-p_4) f_q(\vec{p}) \\ T_2 = & \delta(E_1 + p_1^0) \delta(E_3 + p_3^0) \delta(E_4 - p_4^0) f_{\bar{q}}(-p_1) f_{\bar{q}}(-p_3) f_q(p_4) f_q(\vec{p}) \\ T_3 = & \delta(E_1 + p_1^0) \delta(E_3 - p_3^0) \delta(E_4 + p_4^0) f_{\bar{q}}(-p_1) \bar{f}_q(p_3) \bar{f}_{\bar{q}}(-p_4) f_q(\vec{p}) \\ T_4 = & \delta(E_1 + p_1^0) \delta(E_3 - p_3^0) \delta(E_4 - p_4^0) f_{\bar{q}}(-p_1) \bar{f}_q(p_3) f_q(p_4) f_q(\vec{p}) \\ T_5 = & \delta(E_1 - p_1^0) \delta(E_3 + p_3^0) \delta(E_4 + p_4^0) \bar{f}_q(p_1) f_{\bar{q}}(-p_3) \bar{f}_{\bar{q}}(-p_4) f_q(\vec{p}) \\ T_6 = & \delta(E_1 - p_1^0) \delta(E_3 + p_3^0) \delta(E_4 - p_4^0) \bar{f}_q(p_1) f_{\bar{q}}(-p_3) f_q(p_4) f_q(\vec{p}) \\ T_7 = & \delta(E_1 - p_1^0) \delta(E_3 - p_3^0) \delta(E_4 + p_4^0) \bar{f}_q(p_1) \bar{f}_q(p_3) \bar{f}_{\bar{q}}(-p_4) f_q(\vec{p}) \\ T_8 = & \delta(E_1 - p_1^0) \delta(E_3 - p_3^0) \delta(E_4 - p_4^0) \bar{f}_q(p_1) \bar{f}_q(p_3) f_q(p_4) f_q(\vec{p}).\end{aligned}\quad (4.8)$$

One sees that there are eight terms, or eight processes in this expression. However, due to energy-momentum-conservation T_1, T_2, T_4, T_6 and T_7 vanish, leaving only T_3, T_5 and T_8 . This is a direct consequence of the on-shell nature of the quasiparticle approximation. If this were relaxed, all terms would necessarily have to be included.

We can reorganize this expression into a recognizable physical form by making some simple manipulations. Letting $p_i \rightarrow -p_i$ for the antiquark states and performing the p_1^0, p_3^0, p_4^0 and the p_2 integration by absorbing the appropriate δ -functions, we obtain

$$\begin{aligned}
J_{\text{coll,q}}^{(2)\text{loss}} = & -g^4 m^4 \frac{\pi}{E_p} \int \frac{d^3 p_1}{(2\pi)^3 2E_1} \frac{d^3 p_3}{(2\pi)^3 2E_3} \frac{d^3 p_4}{(2\pi)^3 2E_4} (2\pi)^4 \\
& \times \left\{ \delta^{(4)}(p + p_1 - p_3 - p_4) \bar{f}_q(\vec{p}_1) \bar{f}_q(\vec{p}_3) \bar{f}_q(\vec{p}_4) f_q(\vec{p}) \right. \\
& \quad \times [G^{++}(X, p + p_1) G^{--}(X, p + p_1) + G^{++}(X, p + p_1) G^{--}(X, p - p_3)] \\
& + \delta^{(4)}(p - p_1 + p_3 - p_4) \bar{f}_q(\vec{p}_1) \bar{f}_q(\vec{p}_3) \bar{f}_q(\vec{p}_4) f_q(\vec{p}) \\
& \quad \times [G^{++}(X, p - p_1) G^{--}(X, p - p_1) + G^{++}(X, p - p_1) G^{--}(X, p + p_3)] \\
& + \delta^{(4)}(p - p_1 - p_3 + p_4) \bar{f}_q(\vec{p}_1) \bar{f}_q(\vec{p}_3) f_q(\vec{p}_4) f_q(\vec{p}) \\
& \quad \left. \times [G^{++}(X, p - p_1) G^{--}(X, p - p_1) + G^{++}(X, p - p_1) G^{--}(X, p - p_3)] \right\}.
\end{aligned} \tag{4.9}$$

The first two terms of this expression can be combined if one makes the substitution $p_1 \leftrightarrow p_3$ in the second term. The third term has a symmetry in p_1 and p_3 and can be rewritten as one half the sum of two terms with p_1 and p_3 interchanged. The loss term then becomes

$$\begin{aligned}
J_{\text{coll,q}}^{(2)\text{loss}} = & -g^4 m^4 \frac{\pi}{E_p} \int \frac{d^3 p_1}{(2\pi)^3 2E_1} \frac{d^3 p_3}{(2\pi)^3 2E_3} \frac{d^3 p_4}{(2\pi)^3 2E_4} (2\pi)^4 \\
& \times \left\{ \delta^{(4)}(p + p_1 - p_3 - p_4) \bar{f}_q(\vec{p}_1) \bar{f}_q(\vec{p}_3) \bar{f}_q(\vec{p}_4) f_q(\vec{p}) \right. \\
& \quad \times [G^{++}(X, p + p_1) G^{--}(X, p + p_1) + G^{++}(X, p + p_1) G^{--}(X, p - p_3) \\
& \quad + G^{++}(X, p - p_3) G^{--}(X, p - p_3) + G^{++}(X, p - p_3) G^{--}(X, p + p_1)] \\
& + \delta^{(4)}(p - p_1 - p_3 + p_4) \bar{f}_q(\vec{p}_1) \bar{f}_q(\vec{p}_3) f_q(\vec{p}_4) f_q(\vec{p}) \\
& \quad \times \frac{1}{2} [G^{++}(X, p - p_1) G^{--}(X, p - p_1) + G^{++}(X, p - p_1) G^{--}(X, p - p_3) \\
& \quad + G^{++}(X, p - p_3) G^{--}(X, p - p_3) + G^{++}(X, p - p_3) G^{--}(X, p - p_1)] \left. \right\}.
\end{aligned} \tag{4.10}$$

Using the fact that $[iG^{--}(p)]^\dagger = iG^{++}(p)$ and making the substitution $p_1 \leftrightarrow p_4$ in

the second term, one is able to identify the absolute values squared of the Green functions occurring in $J_{\text{coll,q}}^{(2),\text{loss}}$. One has

$$\begin{aligned}
J_{\text{coll,q}}^{(2),\text{loss}} = & g^4 m^4 \frac{\pi}{E_p} \int \frac{d^3 p_1}{(2\pi)^3 2E_1} \frac{d^3 p_3}{(2\pi)^3 2E_3} \frac{d^3 p_4}{(2\pi)^3 2E_4} (2\pi)^4 \delta^{(4)}(p + p_1 - p_3 - p_4) \\
& \times \left\{ \frac{1}{2} \left| iG^{--}(X, p - p_3) + iG^{--}(X, p - p_4) \right|^2 f_q(\vec{p}) f_q(\vec{p}_1) \bar{f}_q(\vec{p}_3) \bar{f}_q(\vec{p}_4) \right. \\
& \left. + \left| iG^{--}(X, p + p_1) + iG^{--}(X, p - p_3) \right|^2 f_q(\vec{p}) f_{\bar{q}}(\vec{p}_1) \bar{f}_q(\vec{p}_3) \bar{f}_{\bar{q}}(\vec{p}_4) \right\}.
\end{aligned} \tag{4.11}$$

Now one may recognize the scattering amplitude for elastic quark-quark scattering,

$$-i\mathcal{M}_{qq \rightarrow qq}(p1 \rightarrow 34) = (-igm)^2 [iG^{--}(p - p_3) + iG^{--}(p - p_4)], \tag{4.12}$$

and the scattering amplitude for quark-antiquark scattering,

$$-i\mathcal{M}_{q\bar{q} \rightarrow q\bar{q}}(p1 \rightarrow 34) = (-igm)^2 [iG^{--}(p + p_1) + iG^{--}(p - p_3)], \tag{4.13}$$

occurring in Eq.(4.11), which may be concisely written as to give the final result

$$\begin{aligned}
J_{\text{coll,q}}^{(2),\text{loss}} = & \frac{\pi}{E_p} \int \frac{d^3 p_1}{(2\pi)^3 2E_1} \frac{d^3 p_3}{(2\pi)^3 2E_3} \frac{d^3 p_4}{(2\pi)^3 2E_4} (2\pi)^4 \delta^{(4)}(p + p_1 - p_3 - p_4) \\
& \times \left\{ \frac{1}{2} |\mathcal{M}_{qq \rightarrow qq}(p1 \rightarrow 34)|^2 f_q(\vec{p}) f_q(\vec{p}_1) \bar{f}_q(\vec{p}_3) \bar{f}_q(\vec{p}_4) \right. \\
& \left. + |\mathcal{M}_{q\bar{q} \rightarrow q\bar{q}}(p1 \rightarrow 34)|^2 f_q(\vec{p}) f_{\bar{q}}(\vec{p}_1) \bar{f}_q(\vec{p}_3) \bar{f}_{\bar{q}}(\vec{p}_4) \right\}.
\end{aligned} \tag{4.14}$$

The Feynman graphs corresponding to these processes are shown in Figs. 8 and 9 respectively.

2. Quark-gluon scattering cross sections.

We now turn our attention to the graphs of Fig. 6.1 to Fig. 6.4(a), which will lead to scattering processes that involve gluonic degrees of freedom. As in the previous section, the Feynman rules for non-equilibrium processes can be applied to these diagrams and the result Wigner transformed. This results in the following expressions for the self energies,

$$\begin{aligned}
\Sigma_R^{(2)+-}(X, p) = & -g^4 m^4 F_R^2 \int \frac{d^4 p_1}{(2\pi)^4} \frac{d^4 p_2}{(2\pi)^4} \frac{d^4 p_3}{(2\pi)^4} \frac{d^4 p_4}{(2\pi)^4} (2\pi)^4 \delta^{(4)}(p - p_1 - p_2) \\
& \times (2\pi)^4 \delta^{(4)}(p_2 - p_3 - p_4) G^{+-}(X, p_1) S^{++}(X, p - p_3) \\
& \times G^{+-}(X, p_3) S^{+-}(X, p_4) S^{--}(X, p - p_3)
\end{aligned} \tag{4.15}$$

for the rainbow diagram,

$$\begin{aligned}\Sigma_L^{(2)+-}(X, p) = & -\frac{1}{2}g^4m^4F_L^2 \int \frac{d^4p_1}{(2\pi)^4} \frac{d^4p_2}{(2\pi)^4} \frac{d^4p_3}{(2\pi)^4} \frac{d^4p_4}{(2\pi)^4} (2\pi)^4 \delta^{(4)}(p - p_1 - p_2) \\ & \times (2\pi)^4 \delta^{(4)}(p_2 - p_3 - p_4) G^{+-}(X, p_1) G^{++}(X, p_2) \\ & \times G^{+-}(X, p_3) S^{+-}(X, p_4) G^{--}(X, p_2)\end{aligned}\quad (4.16)$$

for the ladder graph,

$$\begin{aligned}\Sigma_{C,(a)/(b)}^{(2)+-}(X, p) = & -g^4m^4F_C^2 \int \frac{d^4p_1}{(2\pi)^4} \frac{d^4p_2}{(2\pi)^4} \frac{d^4p_3}{(2\pi)^4} \frac{d^4p_4}{(2\pi)^4} (2\pi)^4 \delta^{(4)}(p - p_1 - p_2) \\ & \times (2\pi)^4 \delta^{(4)}(p_2 - p_3 - p_4) G^{+-}(X, p_1) G^{\pm\pm}(X, p_2) \\ & \times G^{+-}(X, p_3) S^{+-}(X, p_4) S^{\mp\mp}(X, p - p_3)\end{aligned}\quad (4.17)$$

for the two cloud diagrams, and

$$\begin{aligned}\Sigma_{E,(a)}^{(2)+-}(X, p) = & -g^4m^4F_E^2 \int \frac{d^4p_1}{(2\pi)^4} \frac{d^4p_2}{(2\pi)^4} \frac{d^4p_3}{(2\pi)^4} \frac{d^4p_4}{(2\pi)^4} (2\pi)^4 \delta^{(4)}(p - p_1 - p_2) \\ & \times (2\pi)^4 \delta^{(4)}(p_2 - p_3 - p_4) G^{+-}(X, p_1) S^{++}(X, p - p_4) \\ & \times G^{+-}(X, p_3) S^{+-}(X, p_4) S^{--}(X, p - p_3)\end{aligned}\quad (4.18)$$

for the first exchange diagram. F_R , F_L , F_C and F_E are appropriate color factors, that will be discussed in detail in the following subsection, but which will be suppressed here. Note that a factor $1/2$ occurs in the expression for the ladder diagram because of the gluon loop. The expressions for $\Sigma^{(2)-+}$ are obtained from the ones for $\Sigma^{(2)+-}$ by exchanging $-$ and $+$. To construct the integrated collision term, one has as in the previous section to integrate over p^0 over an interval Δ_{\pm} which contains $\pm E_p(X)$ and one finds, using Eq.(4.1) that the loss term of the collision incorporating the rainbow, cloud, ladder and first exchange graphs, is given as

$$\begin{aligned}J_{\text{coll,g}}^{(2)\text{loss}} = & ig^4m^4 \frac{\pi}{E_p} \int \frac{d^4p_1}{(2\pi)^4} \frac{d^4p_2}{(2\pi)^4} \frac{d^4p_3}{(2\pi)^4} \frac{d^4p_4}{(2\pi)^4} (2\pi)^8 \delta^{(4)}(p - p_1 - p_2) \delta^{(4)}(p_2 - p_3 - p_4) \\ & \times \left\{ S^{++}(X, p - p_3) S^{--}(X, p - p_3) + \frac{1}{2} G^{++}(X, p_2) G^{--}(X, p_2) \right. \\ & + G^{++}(X, p_2) S^{--}(X, p - p_3) + G^{--}(X, p_2) S^{++}(X, p - p_3) \\ & \left. + S^{++}(X, p - p_4) S^{--}(X, p - p_3) \right\} \left(-i\frac{\pi}{E_1}\right) \left(-i\frac{\pi}{E_3}\right) \left(-i\frac{\pi}{E_4}\right) \sum_{i=1}^8 T_i, \quad (4.19)\end{aligned}$$

where

$$\begin{aligned}
T_1 &= \delta(E_1 + p_1^0) \delta(E_3 + p_3^0) \delta(E_4 + p_4^0) f_{\bar{q}}(-p_1) f_{\bar{g}}(-p_3) f_{\bar{g}}(-p_4) f_q(\vec{p}) \\
T_2 &= \delta(E_1 + p_1^0) \delta(E_3 + p_3^0) \delta(E_4 - p_4^0) f_{\bar{q}}(-p_1) f_{\bar{g}}(-p_3) \bar{f}_g(p_4) f_q(\vec{p}) \\
T_3 &= \delta(E_1 + p_1^0) \delta(E_3 - p_3^0) \delta(E_4 + p_4^0) f_{\bar{q}}(-p_1) \bar{f}_g(p_3) f_{\bar{g}}(-p_4) f_q(\vec{p}) \\
T_4 &= \delta(E_1 + p_1^0) \delta(E_3 - p_3^0) \delta(E_4 - p_4^0) f_{\bar{q}}(-p_1) \bar{f}_g(p_3) \bar{f}_g(p_4) f_q(\vec{p}) \\
T_5 &= \delta(E_1 - p_1^0) \delta(E_3 + p_3^0) \delta(E_4 + p_4^0) \bar{f}_q(p_1) f_{\bar{g}}(-p_3) f_{\bar{g}}(-p_4) f_q(\vec{p}) \\
T_6 &= \delta(E_1 - p_1^0) \delta(E_3 + p_3^0) \delta(E_4 - p_4^0) \bar{f}_q(p_1) f_{\bar{g}}(-p_3) \bar{f}_g(p_4) f_q(\vec{p}) \\
T_7 &= \delta(E_1 - p_1^0) \delta(E_3 - p_3^0) \delta(E_4 + p_4^0) \bar{f}_q(p_1) \bar{f}_g(p_3) f_{\bar{g}}(-p_4) f_q(\vec{p}) \\
T_8 &= \delta(E_1 - p_1^0) \delta(E_3 - p_3^0) \delta(E_4 - p_4^0) \bar{f}_q(p_1) \bar{f}_g(p_3) \bar{f}_g(p_4) f_q(\vec{p}). \tag{4.20}
\end{aligned}$$

Once again, eight terms result from this multiplication. Now, again due to energy-momentum-conservation, T_1, T_2, T_3, T_5 and T_8 vanish, and we are left with three non-vanishing terms, T_4, T_6 and T_7 .

Applying the same procedure as for $J_{\text{coll},q}^{(2)\text{loss}}$ as in the previous subsection, one can regroup the remaining terms to read

$$\begin{aligned}
J_{\text{coll},g}^{(2)\text{loss}} &= g^4 m^4 \frac{\pi}{E_p} \int \frac{d^3 p_1}{(2\pi)^3 2E_1} \frac{d^3 p_3}{(2\pi)^3 2E_3} \frac{d^3 p_4}{(2\pi)^3 2E_4} (2\pi)^4 \delta^{(4)}(p + p_1 - p_3 - p_4) \\
&\times \left\{ \frac{1}{2} \left| iG^{--}(X, p + p_1) + iS^{--}(X, p - p_3) + iS^{--}(X, p - p_4) \right|^2 \right. \\
&\quad \times f_q(\vec{p}) f_{\bar{q}}(\vec{p}_1) \bar{f}_g(\vec{p}_3) \bar{f}_g(\vec{p}_4) \\
&\quad + \left| iS^{--}(X, p + p_1) + iG^{--}(X, p - p_3) + iS^{--}(X, p - p_4) \right|^2 \\
&\quad \times f_q(\vec{p}) f_g(\vec{p}_1) \bar{f}_q(\vec{p}_3) \bar{f}_g(\vec{p}_4) \left. \right\}. \tag{4.21}
\end{aligned}$$

In order to identify the physical processes that give rise to these terms, we examine first all possible contributions to the annihilation process $q\bar{q} \rightarrow gg$. The Feynman graphs for this within this model are shown in Fig. 10. The scattering amplitude associated therewith is

$$-i\mathcal{M}_{q\bar{q} \rightarrow gg}(p_1 \rightarrow 34) = (-igm)^2 [iG^{--}(p + p_1) + iS^{--}(p - p_3) + iS^{--}(p - p_4)]. \tag{4.22}$$

In a similar manner, the elastic scattering process $qg \rightarrow qg$, which is shown in Fig. 11, has the scattering amplitude

$$-i\mathcal{M}_{qg \rightarrow qg}(p_1 \rightarrow 34) = (-igm)^2 [iS^{--}(p + p_1) + iG^{--}(p - p_3) + iS^{--}(p - p_4)]. \tag{4.23}$$

One can identify the absolute value squared of Eqs.(4.22) and (4.23) in Eq.(4.21) and therefore $J_{\text{coll,g}}^{(2)\text{loss}}$ can be written as

$$J_{\text{coll,g}}^{(2)\text{loss}} = \frac{\pi}{E_p} \int \frac{d^3 p_1}{(2\pi)^3 2E_1} \frac{d^3 p_3}{(2\pi)^3 2E_3} \frac{d^3 p_4}{(2\pi)^3 2E_4} (2\pi)^4 \delta^{(4)}(p + p_1 - p_3 - p_4) \\ \times \left\{ \frac{1}{2} |\mathcal{M}_{q\bar{q} \rightarrow gg}(p1 \rightarrow 34)|^2 f_q(\vec{p}) \bar{f}_{\bar{q}}(\vec{p}_1) \bar{f}_g(\vec{p}_3) \bar{f}_g(\vec{p}_4) \right. \\ \left. + |\mathcal{M}_{qg \rightarrow qg}(p1 \rightarrow 34)|^2 f_q(\vec{p}) f_g(\vec{p}_1) \bar{f}_q(\vec{p}_3) \bar{f}_g(\vec{p}_4) \right\}. \quad (4.24)$$

The complete loss term is obtained by adding Eq.(4.14) and (4.24),

$$J_{\text{coll}}^{(2)\text{loss}} = J_{\text{coll,q}}^{(2)\text{loss}} + J_{\text{coll,g}}^{(2)\text{loss}}. \quad (4.25)$$

The gain term can be constructed by replacing $f \leftrightarrow \bar{f}$ in the complete loss term. With the relation

$$\frac{d\sigma}{d\Omega} = \frac{|\mathcal{M}|^2}{|\vec{v}_p - \vec{v}_1| 2E_p 2E_1} \frac{dQ}{d\Omega} \quad (4.26)$$

and the phase space factor

$$Q = (2\pi)^4 \delta^{(4)}(p + p_1 - p_3 - p_4) \frac{d^3 p_3}{(2\pi)^3 2E_3} \frac{d^3 p_4}{(2\pi)^3 2E_4}, \quad (4.27)$$

the final form for the Boltzmann equation, calculated to second order in the number of exchanged gluons, is for quarks ($a = q$)

$$2p\partial_X f_a(X, \vec{p}) = \int d\Omega \frac{d^3 p_1}{(2\pi)^3 2E_1} |\vec{v}_p - \vec{v}_1| 2E_p 2E_1 \\ \times \sum_{j=1}^4 s_j \frac{d\sigma_j}{d\Omega} \Big|_{ab \rightarrow cd} \left[\bar{f}_a(\vec{p}) \bar{f}_b(\vec{p}_1) f_c(\vec{p}_3) f_d(\vec{p}_4) - f_a(\vec{p}) f_b(\vec{p}_1) \bar{f}_c(\vec{p}_3) \bar{f}_d(\vec{p}_4) \right], \quad (4.28)$$

where partons b , c , and d can be a quark, antiquark or gluon, and j labels the four processes $j = 1...4$ corresponding to $q\bar{q} \rightarrow gg$, $qg \rightarrow qg$, $qg \rightarrow qg$ and $q\bar{q} \rightarrow q\bar{q}$. The s_j are symmetry factors $s_1 = s_3 = 1/2$ and $s_2 = s_4 = 1$.

The transport equation for gluons can be obtained in an analogous way and calculated for two loops, it takes the same form as Eq.(4.28) with $a = g$. Then j labels the four processes $j = 1...4$ corresponding to $gg \rightarrow gg$, $gg \rightarrow q\bar{q}$, $qg \rightarrow qg$ and $g\bar{q} \rightarrow g\bar{q}$. The appropriate symmetry factors are $s_1 = 1/2$ and $s_2 = s_3 = s_4 = 1$.

B. Color expansion

We now deal with the color factors, which we have neglected so far. We calculate them for *one* $SU(N)$ color group. The overall color factor for both color groups is then obtained by squaring it.

The matrices $(t^a)_{ij}$ are the matrices of the color group in the representation of the quarks, while $(T^a)_{bc} = -if_{abc}$ are the color matrices in the adjoint representation and f_{abc} are the structure constants of the color group, see Eq.(2.2). The t^a 's are normalized to

$$\text{tr}(t^a t^b) = \frac{1}{2} \delta_{ab}. \quad (4.29)$$

The “square” of the generator in some representation must be proportional to the unit operator (Schur’s Lemma). Therefore

$$(t^a)_{ij}(t^a)_{jk} = C_F \delta_{ik} \quad (4.30)$$

and

$$T_{bd}^a T_{dc}^a = f_{bad} f_{cad} = C_A \delta_{bc}, \quad (4.31)$$

where the numbers C_F and C_A are the Casimir operators of the fundamental and adjoint representation, respectively. They take the values (see for example [21])

$$C_F = \frac{N_c^2 - 1}{2N_c} \quad (4.32)$$

and

$$C_A = N_c. \quad (4.33)$$

Consider now the quark self energies that were evaluated in the previous subsection. Let i denote the external parton index. It is therefore not to be summed over. The color factor for the rainbow graph is

$$F_R = t_{ij}^b t_{jk}^a t_{kl}^a t_{li}^b = C_F^2 \delta_{ii} = \frac{(N_c^2 - 1)^2}{4N_c^2} \delta_{ii}. \quad (4.34)$$

For the ladder graph, one finds

$$F_L = (-if_{abc})(-if_{cbd})t_{ij}^a t_{ji}^d = C_A \delta_{ad} t_{ij}^a t_{ji}^d = C_A C_F \delta_{ii} = \frac{N_c^2 - 1}{2} \delta_{ii}. \quad (4.35)$$

For the cloud graph, one obtains

$$F_C = (-if_{acb})t_{ij}^a t_{jk}^b t_{ki}^c = -\frac{N_c^2 - 1}{4}\delta_{ii}, \quad (4.36)$$

where the relation (see for example [21])

$$-if_{abc}t^a t^b = \frac{C_A}{2}t^c \quad (4.37)$$

has been used. The color factor for the exchange graph is

$$F_E = t_{ij}^a t_{jk}^b t_{kl}^a t_{li}^b = -\frac{N_c^2 - 1}{4N_c^2}\delta_{ii}, \quad (4.38)$$

where the relation [21]

$$t^a t^b t^a = \frac{-1}{2N_c}t^b \quad (4.39)$$

has been used. Finally, for the quark loop graph the color factor is given by

$$F_{\text{q-loop}} = t_{ij}^a t_{ji}^b \text{tr}(t^a t^b) = \frac{N_c^2 - 1}{4N_c}\delta_{ii}. \quad (4.40)$$

Up to this point, we have made a semiclassical expansion that involves keeping only the leading term in expanding the exponential in Eq.(2.14) (here the factor \hbar has been set to one.) In addition, we have examined sets of diagrams organized according to the number of interaction lines, i.e. according to the coupling strength. We have found that all graphs in a class are required in order to build up the cross sections that ultimately occur in a Boltzmann like equation. However, at the level of two exchanged gluons, we are already faced with five types of graphs, and this number increases rapidly with the number of exchanged gluons. One possible simplifying assumption is the additional imposition of an expansion in the inverse number of colors. According to such a criterion, the ladder, the rainbow and the cloud diagrams are leading, since their color factors for one color group are of order $O(N_c^2)$ while for the quark-loop diagram it goes as N_c and for the exchange diagram only as N_c^0 .

Since the ladder and the rainbow diagram lead to cross sections involving gluons while the quark-loop diagram leads to elastic quark-(anti)quark cross sections, one can conclude that the quark degrees of freedom are suppressed in comparison with the gluon degrees of freedom. This is in agreement with the results of an evaluation of the quark-quark scattering amplitude within this model [15], in which the quark degrees of freedom are neglected, however due to kinematical reasons.

Although the ladder and the rainbow diagram are both of order $O(N_c^2)$, the ratio of their color factors for one color group is not one, but

$$\frac{F_R}{F_L} = \frac{C_F}{C_A}, \quad (4.41)$$

which is $4/9 \approx 1/2$ for $N_c = 3$. Since in the rainbow diagram the second gluon couples at the quark line while in the ladder diagram it couples at the first gluon, two quark-quark-gluon vertices are suppressed by a factor $4/9$ per color group in comparison with two 3-gluon vertices. Thus, there is no *strict* ordering of the gluon graphs according to a single class of diagrams, in an expansion in $1/N_c$. Although the ladder graphs and the processes that they lead to appear largest, one should not that the symmetry factors of the other graphs compensate for this. A numerical study is essential to determine the actual order of magnitude of each graph.

As a final comment, note that an expansion in color also incorporates the coupling strength. Assuming that $g \sim 1/N_c$, we find that the Fock term $\sim g^2 N_c^2$ and the ladder diagram $\sim g^4 N_c^4$ are of the same order.

C. Three parton production

Since many diagrams contribute to the self energy with three exchanged gluons, we again make an additional expansion in the inverse number of colors as explained in the previous Subsection, and consider only diagrams that do not contain quark loops. In the case of two exchanged gluons, we have seen that the ladder and the rainbow diagrams give rise to the squared scattering amplitudes of *individual* channels. Therefore, we conclude (and will check later) that for the case with three exchanged gluons, the three-rung ladder diagram, the rainbow diagram with three bows and all possible mixtures between them will lead to the squared scattering amplitudes of *individual* channels of processes involving three gluons. The generic form of these diagrams is given in Fig. 12. (Note: diagrams that would generate crossed terms between the single channels are shown in Appendix C).

A direct evaluation of the self energy diagrams in Fig. 12 should give rise to cross sections of processes that involve three gluons, *i.e.* one expects, for example, the three gluon production $q\bar{q} \rightarrow ggg$ but also multiparton production such as $qg \rightarrow qgg$. The generic Feynman diagrams for these processes are shown in Figs. 13 and 14 respectively.

To be specific, let us consider now the ladder diagram of Fig. 12(a), in particular $\Sigma_L^{(3)+-}(X, p)$. There are sixteen possibilities of arranging the signs that can be associated with the vertices of the first and second rungs. Invoking the on-shell argument and energy-momentum conservation, the possibilities become restricted to the single diagram shown in Fig. 15. The explicit expression for this ladder diagram is

$$\begin{aligned} \Sigma_L^{(3)+-}(X, p) = & -i \frac{1}{2} g^6 m^6 \int \frac{d^4 p_1}{(2\pi)^4} \frac{d^4 p_2}{(2\pi)^4} \frac{d^4 p_3}{(2\pi)^4} \frac{d^4 p_4}{(2\pi)^4} \frac{d^4 p_5}{(2\pi)^4} \frac{d^4 p_6}{(2\pi)^4} \\ & \times (2\pi)^4 \delta^{(4)}(p - p_1 - p_2) (2\pi)^4 \delta^{(4)}(p_2 - p_3 - p_4) (2\pi)^4 \delta^{(4)}(p_4 - p_5 - p_6) \\ & \times S^{+-}(X, p_1) G^{++}(X, p_2) G^{+-}(X, p_3) G^{++}(X, p_4) \\ & \times G^{+-}(X, p_5) G^{+-}(X, p_6) G^{--}(X, p_4) G^{--}(X, p_2). \end{aligned} \quad (4.42)$$

Once again, one may insert the quasiparticle *ansätze* for the quark and gluonic Green functions from Eqs.(2.15) - (2.18), and construct the contribution of this ladder term to $J_{\text{coll}}^{(3)\text{loss}}$ as in Subsection IV A by taking its on-shell value

$$J_{\text{coll}}^{(3)\text{loss}} = -i \frac{\pi}{E_p} \Sigma^{(3)+-}(X, p_0 = E_p, \vec{p}) f_q(X, \vec{p}). \quad (4.43)$$

Multiplying out the product of Green functions in terms of the quark and gluonic distribution functions enables us to identify all processes that can occur. The details of this cumbersome calculation are given in Appendix B. Here we simply note that the constraints of energy-momentum conservation admit all processes which have at least two partons in both the initial and final state. That is to say, in addition to the parton production processes $q\bar{q} \rightarrow ggg$ and $qg \rightarrow qgg$, that were already mentioned, one also obtains the matrix elements for the processes $q\bar{q}g \rightarrow gg$ and $qgg \rightarrow qg$.

In order to complete the calculation, the remaining diagrams of Fig. 12 and additional self energy graphs that lead to mixed terms of the scattering amplitudes must be calculated in an analogous way. There are very many such diagrams that build the mixed terms between the scattering amplitudes that were shown in Figs. 13 and 14. For completeness, we show these in Appendix C. We will not however calculate these graphs in any detail here.

The final form of the Boltzmann equation, calculated to third order in the number of exchanged gluons, reads

$$2p \partial_X f_q(X, \vec{p}) = \int \frac{d^3 p_1}{(2\pi)^3 2E_1} \frac{d^3 p_2}{(2\pi)^3 2E_2} \frac{d^3 p_3}{(2\pi)^3 2E_3} (2\pi)^4$$

$$\begin{aligned}
& \times \left\{ \delta^{(4)}(p + p_1 - p_2 - p_3) \sum_{j=1}^4 s_j |\mathcal{M}_j(qa \rightarrow bc)|^2 \right. \\
& \times \left[\bar{f}_q(\vec{p}) \bar{f}_a(\vec{p}_1) f_b(\vec{p}_3) f_c(\vec{p}_4) - f_q(\vec{p}) f_a(\vec{p}_1) \bar{f}_b(\vec{p}_3) \bar{f}_c(\vec{p}_4) \right] \\
& + \int \frac{d^3 p_4}{(2\pi)^3 2E_4} \left\{ \delta^{(4)}(p + p_1 - p_2 - p_3 - p_4) \sum_{j=5}^6 s_j |\mathcal{M}_j(qa \rightarrow bcd)|^2 \right. \\
& \times \left[\bar{f}_q(\vec{p}) \bar{f}_a(\vec{p}_1) f_b(\vec{p}_3) f_c(\vec{p}_4) f_d(\vec{p}_5) - f_q(\vec{p}) f_a(\vec{p}_1) \bar{f}_b(\vec{p}_3) \bar{f}_c(\vec{p}_4) \bar{f}_d(\vec{p}_5) \right] \\
& + \delta^{(4)}(p + p_1 + p_2 - p_3 - p_4) \sum_{j=7}^8 s_j |\mathcal{M}_j(qab \rightarrow cd)|^2 \\
& \times \left[\bar{f}_q(\vec{p}) \bar{f}_a(\vec{p}_1) \bar{f}_b(\vec{p}_3) f_c(\vec{p}_4) f_d(\vec{p}_5) - f_q(\vec{p}) f_a(\vec{p}_1) f_b(\vec{p}_3) \bar{f}_c(\vec{p}_4) \bar{f}_d(\vec{p}_5) \right] \left. \right\}, \\
& \tag{4.44}
\end{aligned}$$

where a, b, c and d are partons and $j = 1...4$ labels the four processes given after Eq.(4.28) while $j = 5...8$ labels the four processes corresponding to $q\bar{q} \rightarrow ggg$, $qg \rightarrow qgg$, $q\bar{q}g \rightarrow gg$ and $qgg \rightarrow qg$. The symmetry factors for $j = 5...8$ are given as $s_5 = 1/3!$ and $s_6 = s_7 = s_8 = 1/2$.

D. n parton production

Of the self energy diagrams of order $O(g^{2n})$, the ladder diagram, the rainbow diagram and all possible mixtures between these two are leading in an expansion in $1/N_c$. On evaluation, these diagrams lead to the scattering process $q\bar{q} \rightarrow ng$ and all possible crossed processes, such as $q\bar{q}g \rightarrow (n-1)g$, $qg \rightarrow q(n-1)g$, ... in which at least two partons occur both in the initial and final states. The Boltzmann equation for quarks then reads

$$\begin{aligned}
p\partial_X f_q(X, \vec{p}) &= \frac{\pi}{E_p} \sum_{m,n=1}^{\infty} \int \frac{d^3 k}{(2\pi)^3 2E_k} \frac{d^3 p_1}{(2\pi)^3 2E_1} \cdots \frac{d^3 p_{m+n}}{(2\pi)^3 2E_{m+n}} (2\pi)^4 \\
& \times \left\{ \delta^{(4)}(p + k + p_1 + \dots + p_{m-1} - p_m - \dots - p_{m+n}) \right. \\
& \times s_{m-1} s_{n+1} |\mathcal{M}(q\bar{q}(m-1)g \rightarrow (n+1)g)|^2 \\
& \times \left[\bar{f}_q(\vec{p}) \bar{f}_{\bar{q}}(\vec{k}) \bar{f}_g(\vec{p}_1) \dots \bar{f}_g(\vec{p}_{m-1}) f_g(\vec{p}_m) \dots f_g(\vec{p}_{m+n}) \right. \\
& \left. \left. - f_q(\vec{p}) f_{\bar{q}}(\vec{k}) f_g(\vec{p}_1) \dots f_g(\vec{p}_{m-1}) \bar{f}_g(\vec{p}_m) \dots \bar{f}_g(\vec{p}_{m+n}) \right] \right. \\
& + \delta^{(4)}(p + p_1 + \dots + p_m - k - p_{m+1} - \dots - p_{m+n}) s_m s_n |\mathcal{M}(qmg \rightarrow qng)|^2 \\
& \times \left[\bar{f}_q(\vec{p}) \bar{f}_g(\vec{p}_1) \dots \bar{f}_g(\vec{p}_m) f_q(\vec{k}) f_g(\vec{p}_{m+1}) \dots f_g(\vec{p}_{m+n}) \right. \\
& \left. \left. - f_q(\vec{p}) f_g(\vec{p}_1) \dots f_g(\vec{p}_m) \bar{f}_q(\vec{k}) \bar{f}_g(\vec{p}_{m+1}) \dots \bar{f}_g(\vec{p}_{m+n}) \right] \right\}
\end{aligned}$$

$$-f_q(\vec{p})f_g(\vec{p}_1)\dots f_g(\vec{p}_m)\bar{f}_q(\vec{k})\bar{f}_g(\vec{p}_{m+1})\dots\bar{f}_g(\vec{p}_{m+n})\Big]\Big\} \quad (4.45)$$

with the symmetry factors $s_n = 1/n!$, which is our final result.

V. SUMMARY AND CONCLUSIONS

In this paper, we have worked out the transport theory for the scalar partonic model. We have placed particular emphasis on the collision term examining the collision integral first in the mean field (Hartree and Fock approximations) and then including more loops. On making an analysis of the color structure, we have found that a $1/N_c$ expansion leads to a suppression of the quark loops and their exchange diagrams, much as occurs in QCD. Thus it turns out that all remaining self energy diagrams that lead to gluon production and quark-gluon scattering are of the same order. We have not been able to find any convincing argument to favor an expansion that only includes ladder graphs, as is for example the dominant contribution in elastic quark-quark scattering in the Regge limit, when considered on its own within this model.

This can simply be traced back to the fact that the uppermost line in the quark or gluon self energy is closed and therefore possesses a momentum that must be integrated over. This fact reemerges in the Boltzmann equation in that all momenta except for that of the particle under study, are integrated over. An additional assumption, e.g. that the uppermost gluonic momentum should take on a specific value, is required in order to generate a leading logarithmic expansion.

We have also analysed the situation involving three loops, which leads to three parton production, and find that initial state interactions also enter into the picture. Finally, a generalized Boltzmann like equation that includes multiple gluon production, but which also incorporates initial state interactions, is given.

In concluding, we comment that further study is required in order to establish the factors that could lead to mass renormalization in this model and which has not yet been addressed.

VI. ACKNOWLEDGMENTS

We wish to thank Klaus Werner at the Ecole des Mines de Nantes for many fruitful discussions and his kind hospitality at this institute while this project was discussed.

APPENDIX A: GREEN FUNCTIONS, TRANSPORT AND CONSTRAINT EQUATIONS

In this appendix, we give a brief guideline for the derivation of the transport and constraint equations, Eqs.(2.8) and (2.9).

The Schwinger-Keldysh Green functions defined in Eqs.(2.5) and (2.6) can be summarized in a compact matrix form

$$\underline{D} = \begin{pmatrix} D^{--} & D^{-+} \\ D^{+-} & D^{++} \end{pmatrix}, \quad (\text{A1})$$

using the generic notation already introduced in Section IIB. From the definition of the Green functions, the relation

$$D^{--}(x, y) + D^{++}(x, y) = D^{-+}(x, y) + D^{+-}(x, y) \quad (\text{A2})$$

follows, showing that the four components D^{ij} are not independent. We define the retarded and advanced Green functions in the standard way as

$$\begin{aligned} D^R(x, y) &:= \Theta(x_0 - y_0)[D^{+-}(x, y) - D^{-+}(x, y)] \\ &= D^{--}(x, y) - D^{-+}(x, y) = D^{+-}(x, y) - D^{++}(x, y) \end{aligned} \quad (\text{A3})$$

$$\begin{aligned} D^A(x, y) &:= -\Theta(y_0 - x_0)[D^{+-}(x, y) - D^{-+}(x, y)] \\ &= D^{--}(x, y) - D^{+-}(x, y) = D^{-+}(x, y) - D^{++}(x, y). \end{aligned} \quad (\text{A4})$$

The equations of motion that the Green functions satisfy are

$$(\square_x + M^2)\underline{D}(x, y) = -\underline{\sigma}_z \delta^{(4)}(x - y) + \int d^4 z \underline{\sigma}_z \underline{\Pi}(x, z) \underline{D}(z, y), \quad (\text{A5})$$

given in terms of the irreducible proper self energy

$$\underline{\Pi} = \begin{pmatrix} \Pi^{--} & \Pi^{-+} \\ \Pi^{+-} & \Pi^{++} \end{pmatrix} \quad (\text{A6})$$

and

$$\underline{\sigma}_z = \begin{pmatrix} 1 & 0 \\ 0 & -1 \end{pmatrix}. \quad (\text{A7})$$

In Eq.(A5), M is the free bosonic parton mass.

The four components of the self energy are also not independent. From their definition, the relation

$$\Pi^{--} + \Pi^{++} = -(\Pi^{+-} + \Pi^{-+}) \quad (\text{A8})$$

can be seen to hold. The retarded and advanced self energies are defined to be

$$\begin{aligned} \Pi^R(x, y) &= \Pi^{--}(x, y) + \Pi^{-+}(x, y) \\ \Pi^A(x, y) &= \Pi^{--}(x, y) + \Pi^{+-}(x, y). \end{aligned} \quad (\text{A9})$$

We now consider specifically the equation of motion for D^{-+} . This reads

$$\begin{aligned} (\square_x + M^2)D^{-+}(x, y) &= \int d^4z \{ \Pi^{--}(x, z)D^{-+}(z, y) + \Pi^{-+}(x, z)D^{++}(z, y) \} \\ &= \int d^4z \{ \Pi^A(x, z)D^{-+}(z, y) - \Pi^{+-}(x, z)D^{-+}(z, y) \\ &\quad + \Pi^{-+}(x, z)D^{+-}(z, y) - \Pi^{-+}(x, z)D^R(z, y) \} \end{aligned} \quad (\text{A10})$$

while the conjugate equation is

$$\begin{aligned} (\square_y + M^2)D^{-+}(x, y) &= - \int d^4z \{ D^{-+}(x, z)\Pi^{++}(z, y) + D^{--}(x, z)\Pi^{-+}(z, y) \} \\ &= \int d^4z \{ D^{-+}(x, z)\Pi^A(z, y) - D^R(x, z)\Pi^{-+}(z, y) \}. \end{aligned} \quad (\text{A11})$$

Now a Wigner transform of both equations is performed to yield

$$\begin{aligned} \left[\frac{1}{4}\square_X - ip\partial_X - p^2 + M^2 \right] D^{-+}(X, p) &= \\ \Pi^A(X, p)\hat{\Lambda}D^{-+}(X, p) - \Pi^{+-}(X, p)\hat{\Lambda}D^{-+}(X, p) \\ + \Pi^{-+}(X, p)\hat{\Lambda}D^{+-}(X, p) - \Pi^{-+}(X, p)\hat{\Lambda}D^R(X, p) \end{aligned} \quad (\text{A12})$$

and

$$\begin{aligned} \left[\frac{1}{4}\square_X + ip\partial_X - p^2 + M^2 \right] D^{-+}(X, p) &= \\ S^{-+}(X, p)\hat{\Lambda}\Sigma^A(X, p) - S^R(X, p)\hat{\Lambda}\Sigma^{-+}(X, p), \end{aligned} \quad (\text{A13})$$

with the differential operator

$$\hat{\Lambda} := \exp \left\{ \frac{-i}{2} \left(\overleftarrow{\partial}_X \overrightarrow{\partial}_p - \overleftarrow{\partial}_p \overrightarrow{\partial}_X \right) \right\}. \quad (\text{A14})$$

Subtracting Eq.(A12) from Eq.(A13) gives the so-called transport equation,

$$-2ip\partial_X D^{-+}(X, p) = I_-, \quad (\text{A15})$$

while adding them yields the so-called constraint equation,

$$\left(\frac{1}{2} \square_X - 2p^2 + 2M^2 \right) D^{-+}(X, p) = I_+, \quad (\text{A16})$$

that were quoted as Eqs.(2.8) and (2.9), and I_{\mp} is as given in Eqs.(2.10) to (2.13).

APPENDIX B: THREE PARTON PRODUCTION

In this Appendix, the explicit evaluation of the ladder graph for three parton production is given. On inserting the quasiparticle Green functions from Eqs.(2.15) to (2.18) in Eq.(4.42) and after performing the $p_2, p_4, p_1^0, p_3^0, p_5^0$ and p_6^0 integration by absorbing the appropriate δ -functions we obtain from Eq.(4.43) the result

$$\begin{aligned} J_{\text{coll}}^{(3)\text{loss}} = & -\frac{1}{2} g^6 m^6 \frac{\pi}{E_p} \int \frac{d^3 p_1}{(2\pi)^3 2E_1} \frac{d^3 p_3}{(2\pi)^3 2E_3} \frac{d^3 p_5}{(2\pi)^3 2E_5} \frac{d^3 p_6}{(2\pi)^3 2E_6} \\ & \times G^{++}(p_3 + p_5 + p_6) G^{--}(p_3 + p_5 + p_6) G^{++}(p_5 + p_6) G^{--}(p_5 + p_6) \\ & \times (2\pi)^4 \delta^{(4)}(p - p_1 - p_3 - p_5 - p_6) \sum_{i=1}^{16} T_i, \end{aligned} \quad (\text{B1})$$

where the T_i are given as

$$\begin{aligned} T_1 &= f_q(\vec{p}) \bar{f}_q(\vec{p}_1) \bar{f}_g(\vec{p}_3) \bar{f}_g(\vec{p}_5) \bar{f}_g(\vec{p}_6) \\ T_2 &= f_q(\vec{p}) \bar{f}_q(\vec{p}_1) \bar{f}_g(\vec{p}_3) \bar{f}_g(\vec{p}_5) f_g(-\vec{p}_6) \\ T_3 &= f_q(\vec{p}) \bar{f}_q(\vec{p}_1) \bar{f}_g(\vec{p}_3) f_g(-\vec{p}_5) \bar{f}_g(\vec{p}_6) \\ T_4 &= f_q(\vec{p}) \bar{f}_q(\vec{p}_1) \bar{f}_g(\vec{p}_3) f_g(-\vec{p}_5) f_g(-\vec{p}_6) \\ T_5 &= f_q(\vec{p}) \bar{f}_q(\vec{p}_1) f_g(-\vec{p}_3) \bar{f}_g(\vec{p}_5) \bar{f}_g(\vec{p}_6) \\ T_6 &= f_q(\vec{p}) \bar{f}_q(\vec{p}_1) f_g(-\vec{p}_3) \bar{f}_g(\vec{p}_5) f_g(-\vec{p}_6) \\ T_7 &= f_q(\vec{p}) \bar{f}_q(\vec{p}_1) f_g(-\vec{p}_3) f_g(-\vec{p}_5) \bar{f}_g(\vec{p}_6) \\ T_8 &= f_q(\vec{p}) \bar{f}_q(\vec{p}_1) f_g(-\vec{p}_3) f_g(-\vec{p}_5) f_g(-\vec{p}_6) \end{aligned}$$

$$\begin{aligned}
T_9 &= f_q(\vec{p}) f_{\bar{q}}(-\vec{p}_1) \bar{f}_g(\vec{p}_3) \bar{f}_g(\vec{p}_5) \bar{f}_g(\vec{p}_6) \\
T_{10} &= f_q(\vec{p}) f_{\bar{q}}(-\vec{p}_1) \bar{f}_g(\vec{p}_3) \bar{f}_g(\vec{p}_5) f_g(-\vec{p}_6) \\
T_{11} &= f_q(\vec{p}) f_{\bar{q}}(-\vec{p}_1) \bar{f}_g(\vec{p}_3) f_g(-\vec{p}_5) \bar{f}_g(\vec{p}_6) \\
T_{12} &= f_q(\vec{p}) f_{\bar{q}}(-\vec{p}_1) \bar{f}_g(\vec{p}_3) f_g(-\vec{p}_5) f_g(-\vec{p}_6) \\
T_{13} &= f_q(\vec{p}) f_{\bar{q}}(-\vec{p}_1) f_g(-\vec{p}_3) \bar{f}_g(\vec{p}_5) \bar{f}_g(\vec{p}_6) \\
T_{14} &= f_q(\vec{p}) f_{\bar{q}}(-\vec{p}_1) f_g(-\vec{p}_3) \bar{f}_g(\vec{p}_5) f_g(-\vec{p}_6) \\
T_{15} &= f_q(\vec{p}) f_{\bar{q}}(-\vec{p}_1) f_g(-\vec{p}_3) f_g(-\vec{p}_5) \bar{f}_g(\vec{p}_6) \\
T_{16} &= f_q(\vec{p}) f_{\bar{q}}(-\vec{p}_1) f_g(-\vec{p}_3) f_g(-\vec{p}_5) f_g(-\vec{p}_6). \tag{B2}
\end{aligned}$$

By attributing unbarred functions f to incoming particles and barred functions \bar{f} to outgoing ones, one can make the identification of T_{16} corresponds with the annihilation process $q\bar{q}ggg \rightarrow \emptyset$, T_1 with $q \rightarrow qggg$, T_8 with $qggg \rightarrow q$ while T_{12} , T_{14} and T_{15} correspond to the process $q\bar{q}gg \rightarrow g$. These processes are all kinematically forbidden. Only processes with at least two partons in both the initial and the final state are kinematically allowed: these are T_2 , T_3 and T_5 , which lead to $qg \rightarrow qgg$, T_4 , T_6 and T_7 , which lead to $qgg \rightarrow qg$, T_{10} , T_{11} and T_{12} , corresponding to $q\bar{q}g \rightarrow gg$, and finally T_9 , which gives rise to $q\bar{q} \rightarrow ggg$.

APPENDIX C: REMAINING SELF ENERGY DIAGRAMS

In Section IIIC, we gave the Feynman graphs which lead to the square of the individual scattering amplitudes. There are many diagrams which give rise to the mixed terms that also are necessary when forming the square of the full amplitude. For completeness, we indicate which generic diagrams also contribute to the self energy $\Sigma^{(3)}$ and lead to these mixed terms between the scattering amplitudes of the individual channels $q\bar{q} \rightarrow ggg$, $qg \rightarrow qgg$, $q\bar{q}g \rightarrow gg$ and $qgg \rightarrow qg$. These are given in Fig. 16. The last six diagrams are not symmetric, and it is to be understood that the mirror reflected diagrams must also be taken into account.

REFERENCES

- [1] See for example, C.-Y. Wong, *Introduction to High-Energy Heavy-Ion Collisions*, (World Scientific, Singapore, 1994).
- [2] K. Geiger and B. Müller, Nucl. Phys. **B369**, 600 (1992).
- [3] K. Geiger and B. Müller, Phys. Rev. D **50**, 337 (1994).
- [4] K. Geiger, Phys. Rev. D **54**, 949 (1996).
- [5] U. Heinz, Phys. Rev. Lett. **51**, 351 (1983); H.-T. Elze and U. Heinz, Phys. Rep. **183**, 81 (1989).
- [6] H.-T. Elze, M. Gyulassy, and D. Vasak, Phys. Lett. **B177** 402 (1986); Nucl. Phys. **276**, 706 (1986).
- [7] W. Botermans and R. Malfliet, Phys. Rep. **198**, 115 (1990).
- [8] K.-C. Chou, Z.-B. Su, B.-L. Hao, and L. Yu, Phys. Rep. **118**, 1 (1985).
- [9] L.D. Landau and E.M. Lifschitz, *Physikalische Kinetik* (Akademie Verlag, Berlin, 1986), Vol.10.
- [10] S. Mrówczyński and U. Heinz, Ann. Phys. (N.Y.) **229** , 1 (1994).
- [11] J.E. Davis and R.J. Perry, Phys. Rev. C **43**, 1893 (1991).
- [12] Y. Nambu and G. Jona-Lasinio, Phys. Rev. **122**, 5 (1961); *ibid* **124**, 246 (1961).
- [13] S.P. Klevansky, A. Ogura, and J. Hüfner, Ann. Phys. (N.Y.) **261**, 261 (1997).
- [14] J.C. Polkinghorne, J. Math. Phys. **4**, 503 (1963); **4**, 1393 (1963); **4**, 1396 (1963).
- [15] J.R. Forshaw and D.A. Ross, *Quantum Chromodynamics and the Pomeron* (Cambridge University Press, Cambridge, 1997).
- [16] U. Heinz, Phys. Rev. Lett. **51**, 94 (1986).
- [17] P.A. Henning, Nucl. Phys. **A546**, 653 (1992).
- [18] P. Rehberg, Phys. Rev. C **57**, 3299 (1998).
- [19] J. Schwinger, J. Math. Phys. **2** , 407 (1961); L.V. Keldysh, JETP **20**, 1018

(1965).

- [20] J.D. Bjorken and S.D. Drell, *Relativistic quantum mechanics* (Mc Graw-Hill, New York, 1964).
- [21] Yu.L. Dokshitzer, in *Lecture Notes in Physics*, edited by F. Lenz, H. Griebhammer, and D. Stoll (Springer-Verlag, Heidelberg, 1997), Vol.496, p.87.

FIGURES

Fig. 1. Closed time path.

Fig. 2. Quark and gluon generic Hartree self energies. Solid lines refer to quarks, wavy lines to gluons.

Fig. 3. Quark and gluon generic one loop self energies. The quark self energy plus the first gluon self energy are Fock diagrams, while (b) of this figure is a polarization insertion.

Fig. 4. Generic diagrams for the quark and gluon self energies that contain two loops.

Fig. 5. The rainbow graphs.

Fig. 6. All diagrams contributing to $\Sigma^{(2)+-}$.

Fig. 7. Diagram of Fig. 6.4b.

Fig. 8. The t and u channel Feynman graphs for elastic quark-quark scattering.

Fig. 9. The s and t channel Feynman graphs for elastic quark-antiquark scattering.

Fig. 10. The s , t and u channel Feynman graphs for the process $q\bar{q} \rightarrow gg$.

Fig. 11. The s , t and u channel Feynman graphs for the process $qg \rightarrow qg$.

Fig. 12. Generic diagrams for the quark self energy that contain three exchanged gluons and which give rise to squared scattering amplitudes for individual channels.

Fig. 13. Feynman graphs for the process $q\bar{q} \rightarrow ggg$.

Fig. 14. Feynman graphs for the process $qg \rightarrow qgg$.

Fig. 15. The only three rung ladder contribution to the quark self energy.

Fig. 16. Generic graphs for the quark self energy that are required for constructing the mixed amplitudes that lead to scatterings with three gluons.

Figure 1

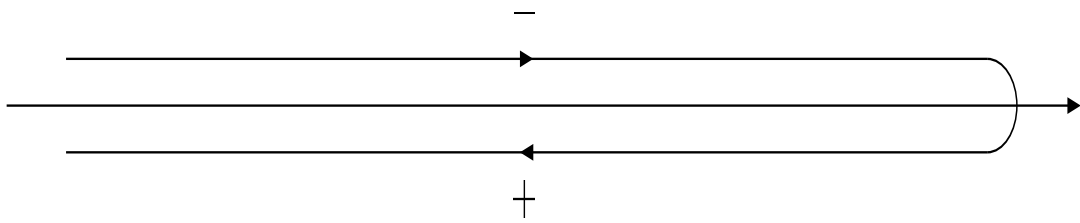


Figure 2

$$\begin{aligned}
 -i\Sigma_q^{--} &= \text{[Diagram 1]} + \text{[Diagram 2]} \\
 -i\Sigma_g^{--} &= \text{[Diagram 3]} + \text{[Diagram 4]}
 \end{aligned}$$

Figure 2 displays two equations relating self-energy terms to Feynman diagrams. The diagrams are organized into two rows, each representing an equation. The first row shows $-i\Sigma_q^{--}$ on the left, followed by an equals sign, then two diagrams separated by a plus sign. The first diagram in the first row consists of a circle with a counter-clockwise arrow, connected to a horizontal line by a vertical wavy line labeled s on its right. The horizontal line has a short horizontal bar underneath it. The second diagram in the first row consists of a circle with a wavy internal line, connected to a horizontal line by a vertical wavy line labeled s on its right. The horizontal line also has a short horizontal bar underneath it. The second row shows $-i\Sigma_g^{--}$ on the left, followed by an equals sign, then two diagrams separated by a plus sign. The first diagram in the second row consists of a circle with a counter-clockwise arrow, connected to a horizontal wavy line by a vertical wavy line labeled s on its right. The horizontal wavy line has a short horizontal bar underneath it. The second diagram in the second row consists of a circle with a wavy internal line, connected to a horizontal wavy line by a vertical wavy line labeled s on its right. The horizontal wavy line also has a short horizontal bar underneath it.

Figure 3

$$\Sigma_{F,q} = \text{---} \overbrace{\text{---}}^{\text{loop}} \text{---}$$

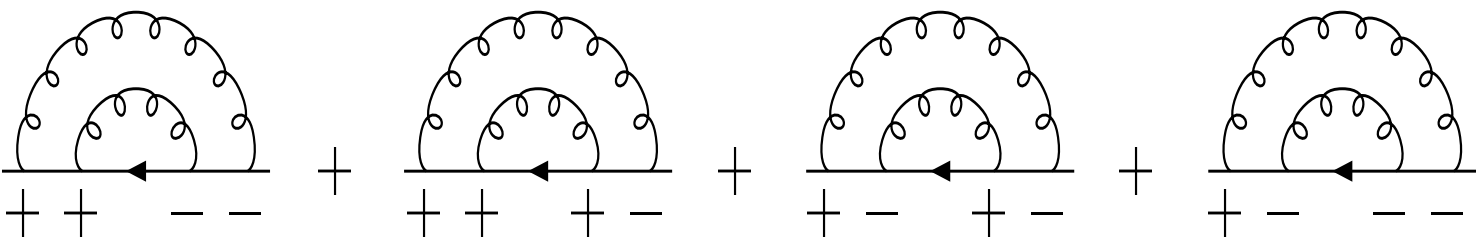
$$\Sigma_{F,g} = \text{---} \text{---} \text{---} + \text{---} \text{---} \text{---}$$

(a)
(b)

Figure 4

$$\begin{aligned}
 -i\Sigma_q^{(2)} = & \text{Rainbow} + \text{Ladder} + \text{Cloud} \\
 & + \text{Exchange} + \text{Quark loop}
 \end{aligned}$$

$$\begin{aligned}
 -i\Sigma_g^{(2)} = & \text{Rainbow} + \text{Exchange} + \text{Quark loop} \\
 & + \text{Quark correction} + \text{Vertex (a)} + \text{Vertex (b)} \\
 & + \text{Vertex (c)}
 \end{aligned}$$

$$-i\Sigma_R^{(2) +-} =$$


The equation shows the sum of four Feynman diagrams. Each diagram has a horizontal line with four external legs. The first two legs are connected by a semi-circular loop with five internal vertices, and the last two legs are connected by a similar semi-circular loop. A horizontal arrow points from the second leg to the third leg. The external legs are labeled with '+' or '-' signs below them. The four diagrams correspond to the four terms in the sum: (+, +, -, -), (+, +, +, -), (+, -, +, -), and (+, -, -, -).

Figure 5

Figure 6

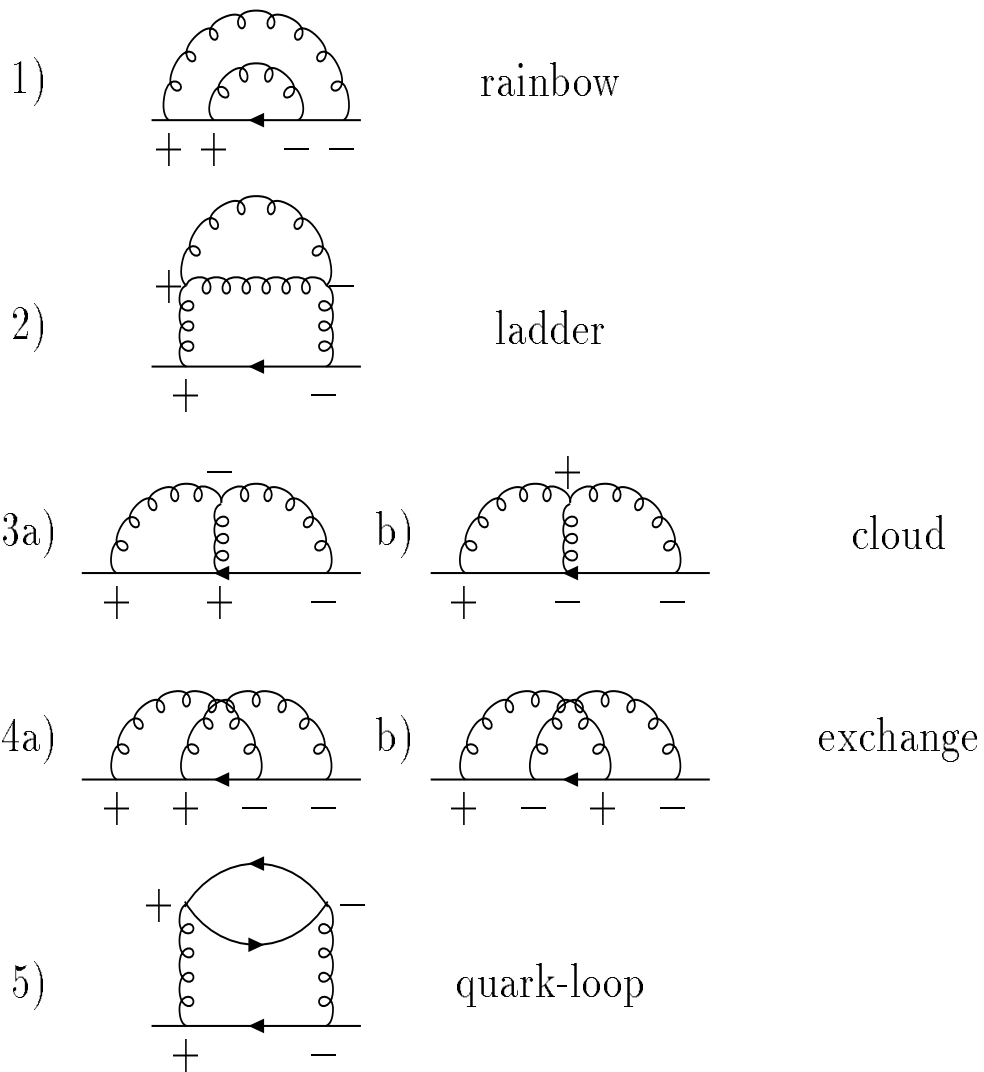


Figure 7

$$4b) = \text{Diagram 1} = \text{Diagram 2}$$

Figure 8

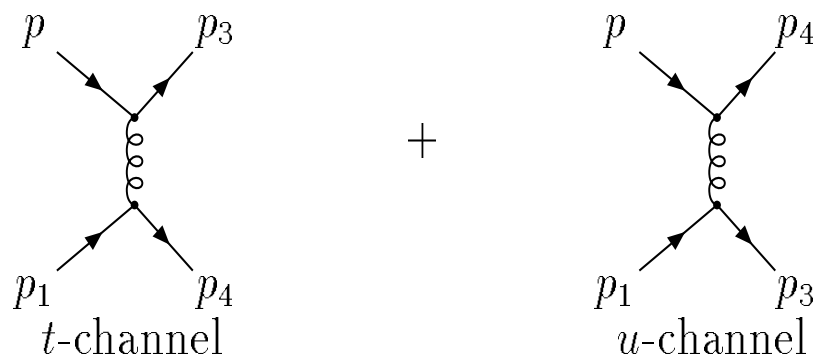


Figure 9

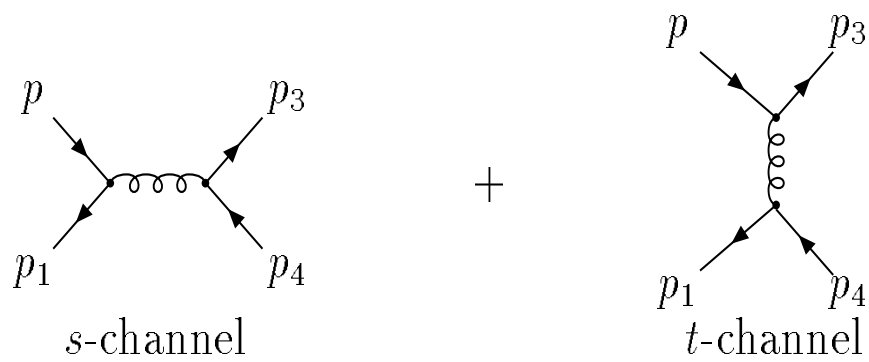


Figure 10

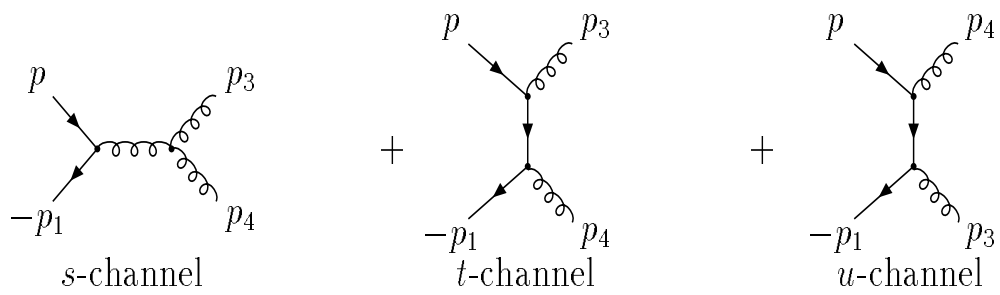


Figure 11

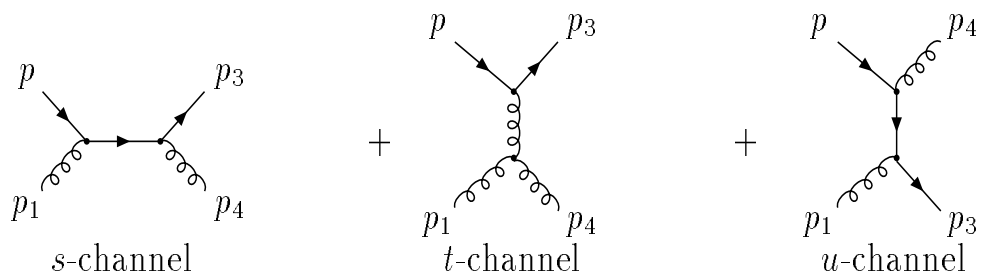


Figure 12

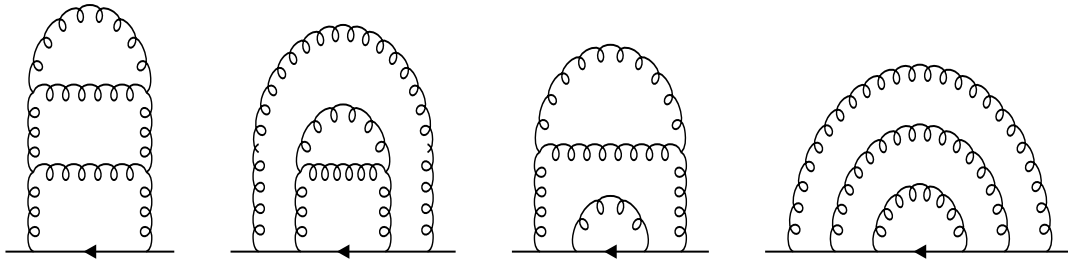
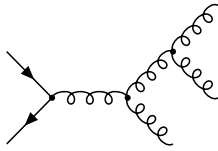
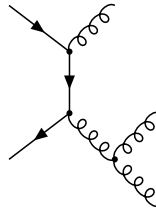


Figure 13



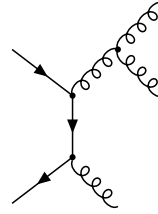
s channel

+

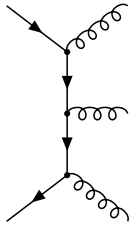


t channel (1)

+



u channel



t channel (2)

Figure 14

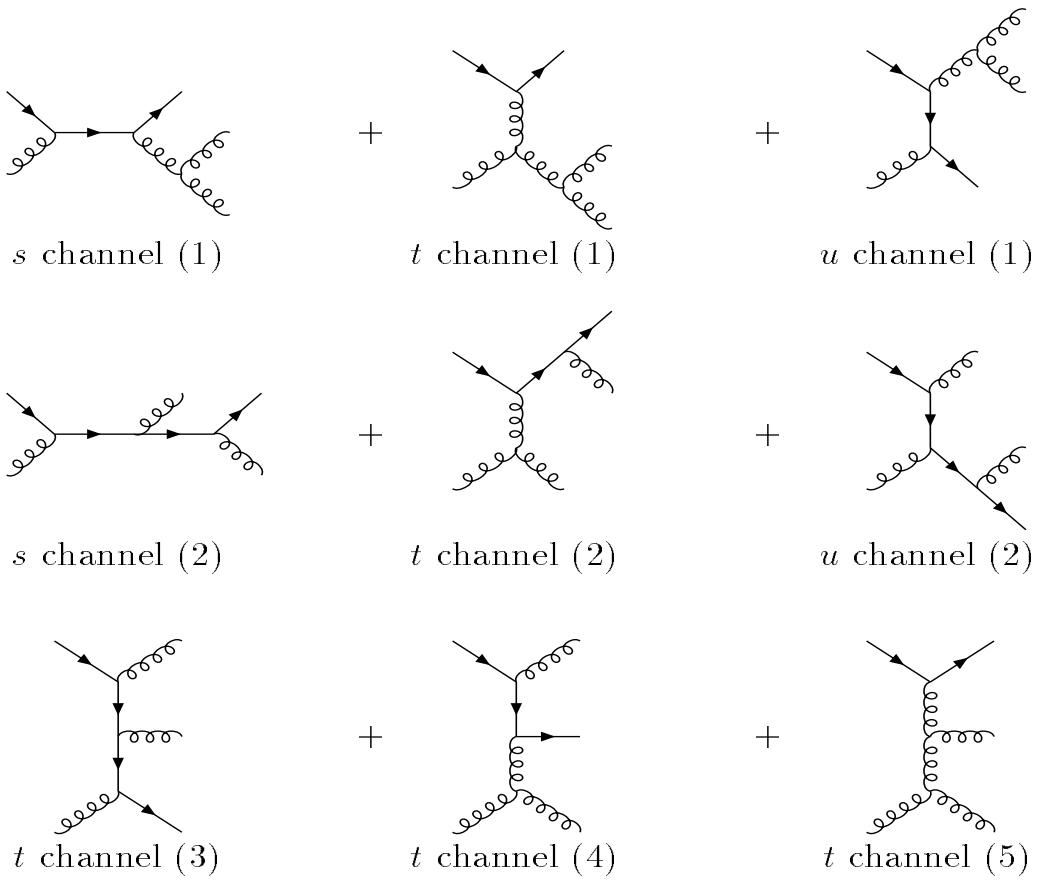


Figure 15

$$-i \Sigma_L^{(3)+-} =$$

Figure 16

